

# Causal effects of chemotherapy regimen intensity on survival outcome in osteosarcoma patients through marginal structural Cox models

Marta Spreafico<sup>\*,1,2</sup>, Cristian Spitoni<sup>3</sup>, Carlo Lancia<sup>1</sup>,  
 Francesca Ieva<sup>2,4</sup>, Marta Fiocco<sup>1,5,6</sup>

<sup>1</sup>Mathematical Institute, Leiden University, Leiden, The Netherlands

<sup>2</sup>MOX – Department of Mathematics, Politecnico di Milano, Milan 20133, Italy

<sup>3</sup>Mathematical Institute, Utrecht University, Utrecht, The Netherlands

<sup>4</sup>Health Data Science Center, Human Technopole, Milan 20157, Italy

<sup>5</sup>Department of Biomedical Data Sciences, Leiden University Medical Center, Leiden, The Netherlands

<sup>6</sup>Trial and Data Center, Princess Máxima Center for Pediatric Oncology, Utrecht, The Netherlands

\*[m.spreafico@math.leidenuniv.nl](mailto:m.spreafico@math.leidenuniv.nl)

## Abstract

As patients develop toxic side-effects, cancer treatment is adapted over time by either delaying or reducing the dosage of the next chemotherapy course. Being at the same time risk factors for mortality and predictors of future exposure levels, toxicities represent time-dependent confounders for the effect of chemotherapy on patient's survival. In the presence of confounders, classical survival approaches have limitations in causally interpreting the hazard ratio of the treatment, even when randomized. The Intention-To-Treat approach is widely used in chemotherapy studies, although it is far from representing everyday clinical practice. Marginal Structural Cox Models (Cox MSMs) in combination with Inverse Probability of Treatment Weighting (IPTW) are a proper tool to evaluate the causal effects of an exposure on survival outcomes. In this work, using novel definitions of Received Dose Intensity and Multiple Overall Toxicity, suitable IPTW-based techniques and Cox MSMs are designed to mimic a randomized trial where chemotherapy joint-exposure is no longer confounded by toxicities. In this pseudo-population, a crude analysis suffices to estimate the causal effect of joint-exposure modifications. This paper discusses an innovative and detailed analysis of complex chemotherapy data, with tutorial-like explanations about the difficulties encountered and the novel problem-solving strategies deployed. This work highlights the confounding nature of toxicities and shows the detrimental effect of not considering them in the analyses. To the best of our knowledge, this is the first study combining different methodologies in an innovative way to eliminate the *toxicity-treatment-adjustment* bias in chemotherapy trial data.

**Key-words:** Marginal Structural Cox Models; Inverse Probability of Treatment Weighting; Received Dose Intensity; Chemotherapy; Event-Free Survival

# 1 Introduction

Osteosarcoma is a rare malignant bone tumour mainly affecting children and young adults with an annual incidence of 3-4 patients per million.<sup>1</sup> Multidisciplinary management including neoadjuvant and adjuvant chemotherapy with aggressive surgical resection<sup>2</sup> or intensified chemotherapy has improved clinical outcomes but over the past 40 years there have been no further improvements in survival.<sup>3</sup> The strongest prognostic factor of both event-free and overall survival known so far in osteosarcoma is Histological Response (HRe),<sup>4</sup> i.e., improvement in the appearance of microscopic tissue specimens in a patient after pre-operative chemotherapy. The impact of chemotherapy dose modification on patients' survival is still unclear.<sup>5</sup>

In cancer trials, the relationship between chemotherapy regimen intensity and survival is problematic to analyse due to the presence of negative feedback between exposure to cytotoxic drugs and consequent toxic side effects. For this reason, chemotherapy is usually modelled by different allocated regimens, i.e., by Intention-To-Treat (ITT) analysis.<sup>6</sup> Since ITT ignores anything that happens after randomization, such as protocol deviations or changes in drug intake over time,<sup>7</sup> Received Dose Intensity (RDI)<sup>8</sup> indicator has been introduced to investigate how *actual* and *planned* treatment differ. This new approach marks a significant departure from ITT in the direction of a more precise description of the actual clinical practice. Lancia *et al.* (2019)<sup>5</sup> showed that there is mismatch between target and achieved chemotherapy-RDI in osteosarcoma due to toxic side effects developed by patients through therapy. Toxicities affect subsequent exposure by delaying the next cycle or reducing chemotherapy doses,<sup>9</sup> representing one of the main reasons for treatment discontinuation.<sup>10</sup> Being at the same time risk factors for mortality and predictors of future exposure levels, toxicities represent *time-dependent confounders* for the effect of chemotherapy on patient's survival. In the presence of confounders, classical survival approaches<sup>11-13</sup> have limitations in causally interpreting the hazard ratio of the treatment variable, even if the treatment is randomized.<sup>14</sup>

Time-dependent confounding of the exposure-outcome association represents a specific challenge for estimating treatment effect on the outcome of interest. Standard analyses fail to give consistent estimators in the presence of time-varying confounders if they are affected by treatment.<sup>15</sup> Several statistical methods to control for exposure-affected time-varying confounders have been proposed, including, among others, g-computation formula,<sup>16</sup> g-estimation of structural nested models<sup>17</sup> or Marginal Structural Models (MSMs) estimated using Inverse Probability of Treatment Weighting (IPTW).<sup>18</sup> In case of time-to-event outcomes, marginal structural Cox model (Cox MSM) is by far the most commonly used method in practice.<sup>19</sup>

Cox MSMs were introduced by Hernán *et al.* (2000)<sup>20</sup> to estimate the causal effect of therapy modifications on survival in presence of time-dependent confounders through IPTW. Making use of marginal (population average) rather than conditional hazard models,<sup>21</sup> Cox MSMs target *counterfactual* time-to-event variables, that is the time at which an event would have been observed if patient had been administered – *possibly contrary to fact* – a specific exposure level. IPTW is a propensity score-based method which creates a pseudo-population by weighting each subject with the inverse probability of observing a certain treatment allocation given past exposure and confounders. In such pseudo-population, confounders no longer predict exposure and the causal effects of treatment modifications on survival can be estimated by a crude analysis. IPTW construction requires a thoughtful process to determine an adequate set of confounding covariates which enter into the decision-making process of allocating treatment modifications. For this set of confounders, the four main assumptions of causal inference with MSM (i.e., no unmeasured confounding, consistency, positivity, no misspecification of the model)<sup>22</sup> must be satisfied.<sup>23</sup> Compared to a standard propensity score matching, IPTW has the advantages of considering more than two treatment comparisons and retaining all eligible patients in the analysis, which may be preferred for small

sample size.<sup>24</sup>

Motivated by a clinical question concerning the effect of changes in therapy intensity on survival for osteosarcoma patients, this paper proposes an innovative approach exploiting treatment-administration data to assess the causal effect of chemotherapy-exposure on Event-Free Survival (EFS). Data from the control arms of two clinical trials of chemotherapy in osteosarcoma, namely, European Osteosarcoma Intergroup studies BO03<sup>25</sup> and BO06<sup>26</sup> (European Organisation for Research and Treatment of Cancer (EORTC) 80861 and 80931, respectively) are analysed. These data are complex because the drug administration is longitudinal while only the most severe side-effects are recorded. The analysis of these mixed longitudinal/non-longitudinal data requires the combination of several methodologies within a new analytical strategy considering all aspects peculiar to the chemotherapy process. IPTW-based techniques and Cox MSMs are used to mimic a randomized trial where joint-exposure intensity is no longer confounded by toxicities or other confounders, and a crude analysis suffices to estimate the causal effect of exposure modifications. This requires (i) a proper (time-dependent) definition of the joint-exposure, (ii) a tailor-made identification of all possible (time-dependent) confounders, and (iii) a proper characterisation of the causal structure of the chemotherapy data. New definitions of joint-exposure, based on *time-fixed final RDI* or *time-dependent pre/post-operative RDI*<sup>25</sup> combined with HRe, are proposed along with the confounding factors and Direct Acyclic Graphs (DAGs)<sup>22,27</sup> to describe the causal exposure-confounders-outcome structure. Since adjustments in treatment allocation are determined by the overall toxic burden of each patient, the different types and number of side effects must be adequately summarized and quantified. The new longitudinal Multiple Overall Toxicity (MOTox) score introduced by Spreafico *et al.* (2021)<sup>28</sup> is hence adapted to the data under study. This allows multiple toxicities to be included within the causal structure identified by DAGs in a novel way. To the best of our knowledge, this is the first study of IPTW-based techniques applied to survival data from chemotherapy-randomized trials in order to eliminate the *toxicity-treatment-adjustment* bias.

The aim of this paper is to introduce an innovative and detailed RDI-based analysis of complex chemotherapy data, along with tutorial-like explanations of the difficulties present in this context and the novel problem-solving strategies proposed. Data from BO03 and BO06 trials are presented in Section 2. The process of building proper causal models based on joint-exposure (difficult due to lack of longitudinal confounders) using two alternative strategies is shown in Section 3. Section 4 discusses the Cox MSMs results, in contrasts to the standard Cox models fitted on the unweighted original population. The article ends with a discussion in Section 5.

## 2 Data description

In Section 2.1 the selected cohort of patients from BO03 and BO06 trials is illustrated. Longitudinal chemotherapy data and patient characteristics are presented in Section 2.2.

### 2.1 Cohort selection

Data from control arms of European Osteosarcoma Intergroup (EOI) randomised clinical trials BO03 and BO06 (EORTC 80861 and 80931, respectively) were analysed. In both trials, control arms were characterized by the standard EOI treatment structured in 6 cycles of 3-weekly Cisplatin (CDDP) ( $100 \text{ mg/m}^2$ ) plus Doxorubicin (DOX) ( $75 \text{ mg/m}^2$ ), and compared to a different therapy regimen (i.e., variant of Rosen's T10 regimen<sup>29</sup> in BO03 and a 2-weekly intensified version of CDDP+DOX<sup>26</sup> in BO06). Results of the primary analyses on BO03 and BO06 data can be found in Lewis *et al.* (2000; 2007).<sup>25,26</sup>

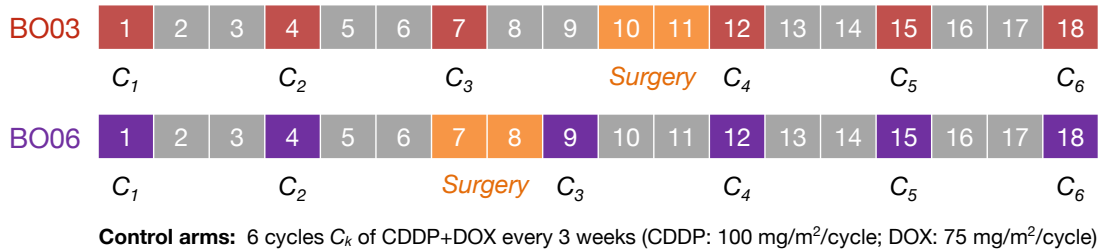


**Figure 1:** Control arms design for BO03 and BO06 randomised clinical trials, characterized by the standard European Osteosarcoma Intergroup treatment structured in 6 cycles of 3-weekly Cisplatin (CDDP) (100 mg/m<sup>2</sup>) plus Doxorubicin (DOX) (75 mg/m<sup>2</sup>).

As the control arms design in Figure 1 shows, in both trials chemotherapy was administered before and after surgical removal of the primary osteosarcoma. At the end of the pre-operative treatment, with a nominal duration of 3 cycles in BO03 and 2 in BO06, the tumour was surgically resected, and the levels of tumour necrosis and Histological Response (HRe) evaluated. Variations to the planned surgery-schedule happened quite often due to administrative reason (delayed surgery) or disease progression (premature surgery), in a small number of cases surgery was delayed due to haematological toxicity (low platelets count). Post-operative chemotherapy was intended to resume 2 weeks after surgery.

In total 444 patients were enrolled in the control arms of BO03 (199) and BO06 (245). In this sample, 106 (23.9%) patients were excluded due to missing HRe. Of the remaining 338 patients, 58 subjects stopped the chemotherapy treatment or did not undergo surgery, while 4 completed the treatment but experienced an event during its administration. The final cohort of 276 patients (114 from BO03 and 162 from BO06, respectively) included in the analyses (62.2% of the initial sample) is shown in the consort diagram in Appendix A.

## 2.2 Complexity of chemotherapy data

In cancer trials, therapy administration is usually complicated by the dynamical adjustment of the treatment on patients' clinical picture. Exposure to chemotherapy is likely to produce multi-systemic side effects, e.g. organ toxicity or myelosuppression. These side effects are a threat to patient's life and must be controlled by allocating either dose reductions/discontinuations or delays in the administration of the next course.<sup>9</sup>

In BO03 and BO06 trials, case report forms were used to document across cycles all the information required by protocols for each patient. Patients baseline characteristics (age, gender, allocated chemotherapy regimen, site and location of the tumour) were registered at randomization. Therapy starting day was usually on the day of randomization or the day after, but could be postponed in case of administrative or clinical reasons. Patient and trial characteristics over the entire dataset and by each trial are shown in Table 1.

Treatment-related factors (administered dose of chemotherapy, cycles delays, haematological parameters, chemotherapy-induced toxicity and histological response to pre-operative chemotherapy) were collected prospectively during therapy. In both studies, toxic side effects were recorded using the Common Terminology Criteria for Adverse Events Version 3 (CTCAE v3.0),<sup>30</sup> with grades ranging from 0 (none) to 4 (life-threatening) (see Appendix B for further details). Toxicity were collected longitudinally in BO06 trial, whereas in BO03 only the highest CTCAE grade (i.e., the most severe) was recorded for each toxicity in both the pre-operative and post-operative peri-

**Table 1:** Patients baseline and trial characteristics.

	All	BO03	BO06
<b>Patients</b>	276	114 (41.3%)	162 (58.7%)
<b>Age [years]</b>			
<i>child</i> *	76 (27.5%)	26 (22.8%)	50 (30.9%)
<i>adolescent</i> *	117 (42.4%)	49 (43.0%)	68 (42.0%)
<i>adult</i> *	83 (30.1%)	39 (34.2%)	44 (27.1%)
Median [IQR]	15.1 [11.7;18.2]	16.0 [12.8;19.0]	14.6 [11.3;17.7]
Min/Max	3.6/37.5	4.7/32.6	3.6/37.5
<b>Gender</b>			
<i>Female</i>	109 (39.5%)	43 (37.7%)	66 (40.7%)
<i>Male</i>	167 (60.5%)	71 (62.3%)	96 (59.3%)
<b>Starting day**</b>			
<i>on time</i> (day 0-1)	196 (71.0%)	63 (55.3%)	133 (82.1%)
<i>low-delay</i> (day 2-3)	43 (15.6%)	23 (20.2%)	20 (12.3%)
<i>delay</i> (day $\geq$ 4)	37 (13.4%)	28 (24.5%)	9 (5.6%)
Median [IQR]	1 [0;2]	1 [0;3]	0 [0,1]
Min/Max	0/15	0/15	0/7
<b>Surgery time‡</b>			
<i>on time</i>	80 (29.0%)	29 (25.4%)	51 (31.5%)
<i>delayed</i>	196 (71.0%)	85 (74.6%)	111 (68.5%)
Median [IQR]	11 [4;22]	14 [5.25;22]	10 [4;21]
Min/Max	-39/132	-39/103	-3/132

\* Age groups were defined according to Collins *et al.* (2013):<sup>31</sup> *child* (male: 0–12 years; female: 0–11 years), *adolescent* (male: 13–17 years; female: 12–16 years) and *adult* (male: 18 or older; female: age 17 years or older).

\*\* Starting day since randomization date. P-value of two-sided Mann-Whitney U test for starting day in BO03 vs BO06: 7.571e-08; p-value of chi-squared test among starting day category and trial: 1.096e-06.

‡ Surgery time (i.e., days since start of the first cycle) with respect to schedule is considered *on time* if performed from at most at the end of the scheduled week (BO03: week 10 – day 63 since start of first cycle; BO06: week 7 – day 42 since start of first cycle), or *delayed* if performed 7 or more days after scheduled date. P-value of two-sided Mann-Whitney U test for surgery time wrt schedule in BO03 vs BO06: 0.0899; p-value of chi-squared test among surgery time category and trial: 0.3397.

ods. According to protocols, the following side effects were linked to specific dose reduction or delay rules: *leucopenia*, *thrombocytopenia*, *oral mucositis*, *ototoxicity*, *cardiotoxicity* and *neurotoxicity*. If different *rule-specific* conditions co-existed and more than one dose reduction (or cumulative delays) applied, the lowest dose (or the highest delays) calculated was employed. According to expert knowledge, although not directly related to a specific adjustment rule, patient’s *generic* conditions of *nausea/vomiting* and *infections* was also taken into account during therapy. Treatment adjustments were hence determined as a combination of overall toxic burden related to both rule-specific and generic conditions, representing the confounding mechanisms due to toxicities.

To let pre- and post-operative toxicities be properly accounted as confounding covariates and included in the analyses, individual side effects had to be appropriately summarized in order to quantify the overall toxic burden. In fact, in case of multiple adverse events, treatment was adapted according to patient’s overall toxic burden rather individual CTCAE grades for the various toxicities. For this purpose, the new longitudinal Multiple Overall Toxicity (MOTox) score introduced by Spreafico *et al.* (2021)<sup>28</sup> can be exploited. The rationale behind this longitudinal min-max index was to include three important components of adverse events in the MOTox score: (i) multiple lower-grade chronic toxicities (which may have an impact on the patient’s quality of life); (ii) huge level in a specific toxicity (which may cause severe effects and permanent consequences

for the patient); (iii) time dependency.<sup>28</sup> Since toxicity data over cycles were not recorded for the BO03 trial, MOTox computation was based on pre- and post-operative periods, by considering the highest CTCAE grade recorded for each toxicity during pre/post-operative cycles.

**Multiple Overall Toxicity score.** Let  $\mathcal{M}$  and  $k$  denote the set of different toxicities and the time-period index, respectively. Let  $tox_{i,k}^m$  (with value from 0 to 4) be the most severe CTCAE grade of the  $m$ -th toxicity (with  $m = 1, \dots, |\mathcal{M}|$ ) measured during period  $k$  for the  $i$ -th patient. The Multiple Overall Toxicity (MOTox) score for the  $i$ -th patient during period  $k$  is defined as:

$$MOTox_{i,k} = \frac{1}{|\mathcal{M}|} \sum_{m=1}^{|\mathcal{M}|} tox_{i,k}^m + \max_{m=1, \dots, |\mathcal{M}|} (tox_{i,k}^m).$$

In particular, for each patient  $i$  four different MOTox scores can be computed considering as time-period index the pre- and post-operative periods, i.e.,  $k \in \{pre, post\}$ , and two disjoint sets of toxicities related to *rule-specific* and *generic* conditions, i.e.,  $\mathcal{M}^{(rule)} = \{leucopenia, thrombocytopenia, oral mucositis, ototoxicity, cardiotoxicity, neurotoxicity\}$  and  $\mathcal{M}^{(gen)} = \{nausea, infection\}$ .

Figure 2 displays a summary of pre/post-operative MOTox characteristics for both *rule-specific* (left panel) and *generic* (right panel) conditions. *Generic* MOTox scores were high: pre/post-operative median MOTox values were equal to 4.5; this means that in median patients experienced at least one generic side effect of CTCAE-grade 3 (i.e., severe or medically significant). This is not surprising because nausea is the most common chemotherapy-induced adverse event. *Rule-specific* MOTox resulted higher in the post-operative period than in the pre-surgery one. This indicates that toxicity levels have accumulated over time resulting in more severe overall toxic burden in the second phase of treatment.

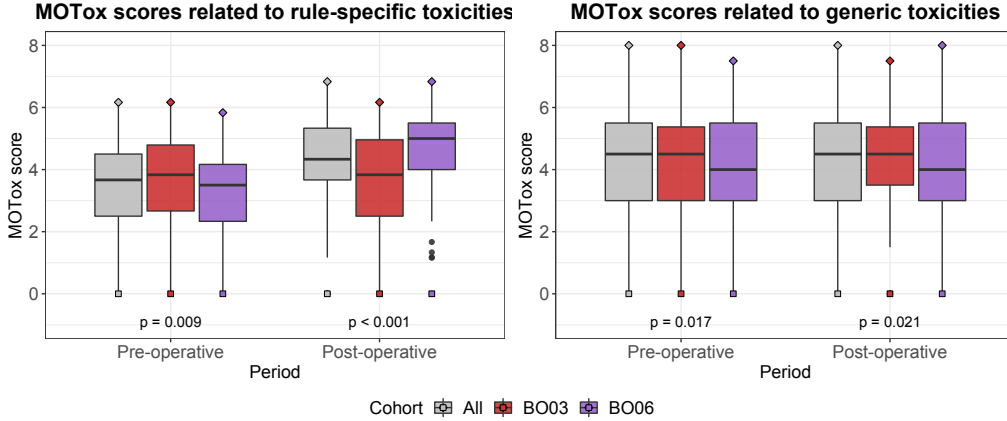


**Figure 2:** Left panel: boxplots of pre-operative and post-operative MOTox scores related to *rule-specific* toxicities, i.e.,  $MOTox_{i,k}^{(rule)}$  with  $k \in \{pre, post\}$  and  $\mathcal{M}^{(rule)} = \{leucopenia, thrombocytopenia, oral mucositis, ototoxicity, cardiotoxicity, neurotoxicity\}$ . Right panel: boxplots of pre-operative and post-operative MOTox scores related to *generic* toxicities, i.e.,  $MOTox_{i,k}^{(gen)}$  with  $k \in \{pre, post\}$  and  $\mathcal{M}^{(gen)} = \{nausea, infection\}$ .

Boxplots are grouped by cohorts (gray: *All*; red: *BO03*; purple: *BO06*). Squares and diamonds represent minimum and maximum values, respectively. P-values  $p$  refer to Mann-Whitney U tests for the distribution of MOTox scores in BO03 vs BO06 cohorts.

### 2.2.1 Chemotherapy exposure characteristics

Data on chemotherapy administration (administered dose of chemotherapy, cycle starting dates, delays) were collected at each treatment cycle in both trials. After pre-operative treatment, surgery was performed and data about Histological Response (HRe) were provided. Chemotherapy exposure can be evaluated in terms of both (i) reductions in the actual dose intensity with respect to anticipated/planned one (i.e., by RDI reduction) and (ii) “good” or “poor” response to pre-operative treatment (i.e., by HRe) classified according to the level of tumour necrosis assessed after surgical resection (planned at the end of cycle 3/2 in BO03/BO06 – see Figure 1).

As mentioned in Section 2.1, control arm patients in both BO03 and BO06 underwent the standard EOI treatment structured in 6 cycles of 3-weekly CDDP plus DOX. Reductions of CDDP and/or DOX dosage at each cycle may be assessed considering the *cycle-standardized (received) dose*. In the following definitions,  $i$  and  $j$  denote the patient and the cycle, respectively.

**Cycle-standardized dose:**

$$\delta_{ij}^d = \frac{\text{actual dose of drug } d \text{ assumed at cycle } j \text{ by patient } i \text{ [mg/m}^2\text{]}}{\text{anticipated dose of drug } d \text{ [mg/m}^2\text{]}} \quad (1)$$

where  $d$  is the type of drug (CDDP or DOX). As described in the trial protocols (see Figure 1), anticipated doses of CDDP and DOX are  $100 \text{ mg/m}^2$  and  $75 \text{ mg/m}^2$ , respectively.

Figure 3 shows the longitudinal nature of drug-dosage data and how treatment modifications were implemented in the two studies. Reductions were usually allocated in the last cycles. This is in line with the common understanding that toxicity levels are more severe towards the end of the treatment and tend to cumulate over time.

To evaluate both dose reductions/discontinuations, time-delays, and their impact in reducing the intensity of the whole therapy, the so-called Received Dose Intensity<sup>5,8,25</sup> approach can be adopted. This method is able to summarize information on treatment adjustments during the whole therapy, considering both *standardized (received) dose* and *time*.<sup>25</sup>

**Standardized dose:**

$$\Delta_i = \frac{1}{2} (\Delta_i^{CDDP} + \Delta_i^{DOX}) = \frac{1}{12} \left( \sum_{j=1}^6 \delta_{ij}^{CDDP} + \sum_{j=1}^6 \delta_{ij}^{DOX} \right) \quad (2)$$

where 6 is the total number of cycles for the whole treatment.  $\Delta_i < 1$  indicates dose-reduced therapies, whereas  $\Delta_i > 1$  corresponds to dose-augmented therapies.

**Standardized time:**

$$\Gamma_i = \frac{\text{actual treatment time}}{\text{anticipated treatment time}} \quad (3)$$

where

- *actual treatment time* is the difference in days between the starting date of cycle 1 and the 3rd day after the start of cycle 6,
- *anticipated treatment time* is  $21 \times 5 + 14 + 3 = 122$  days, i.e., 5 cycles lasting 21 days each, 14 days of surgery and 3 days after the start of cycle 6.

$\Gamma_i > 1$  indicates delayed therapies, whereas  $\Gamma_i < 1$  corresponds to compressed treatments.

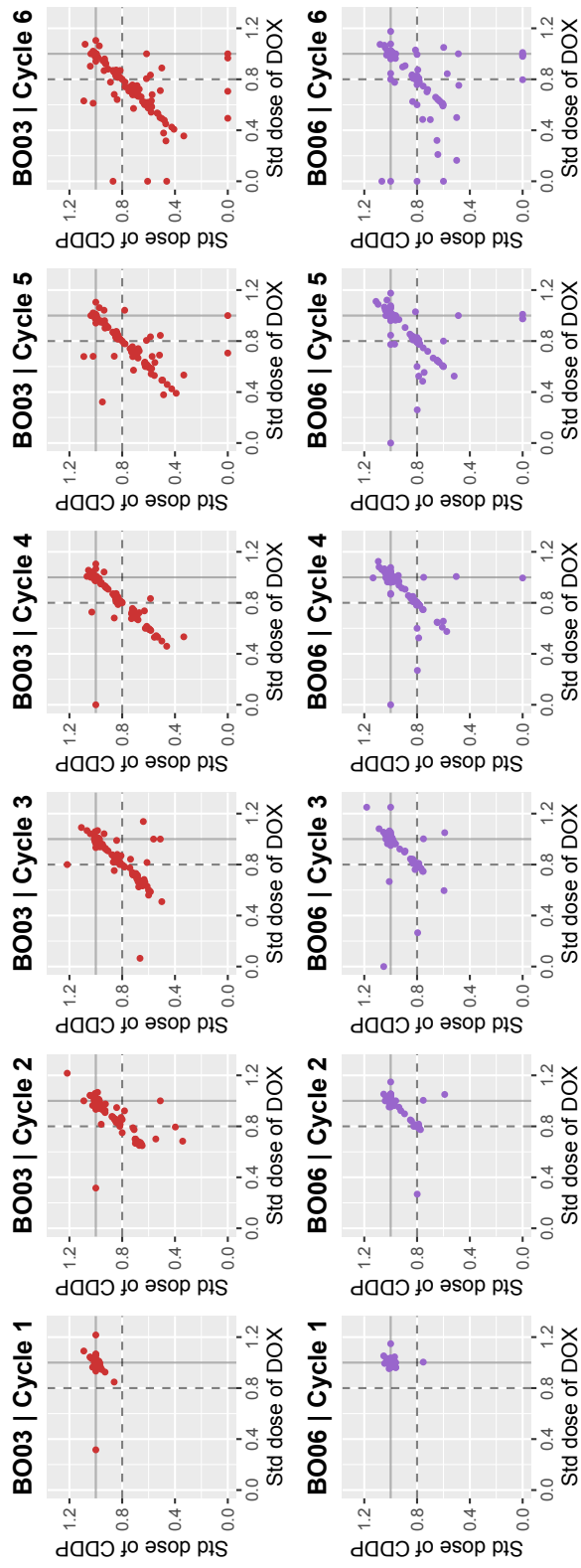


**Figure 3:** Scatter plots of cycle-standardised CDDP-dose ( $\delta_{ij}^{CDDP}$ ) vs. cycle-standardised DOX-dose ( $\delta_{ij}^{DOX}$ ) over cycles  $j = 1, \dots, 6$  (see Equation (1)) conditional on cycle and trial (*BO03*: top panels; *BO06*: bottom panels). Solid lines mark the planned dose, while dotted lines mark reductions of 20%. In order to improve the readability of the plot, very large values are trimmed off to 1.25.

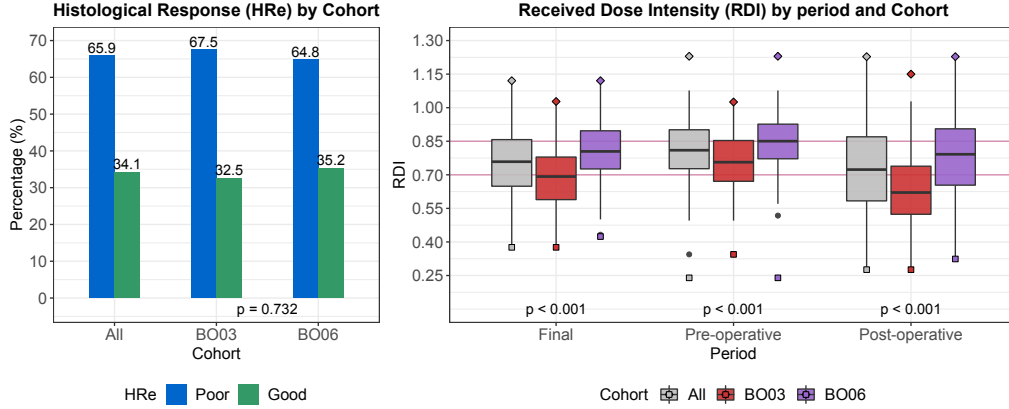


**Figure 4:** Patients treatment exposure characteristics. Left panel: barplots of Histological Response (HRe) by cohort (All, BO03, BO06) coloured according to HRe level (blue: *poor*; green: *good*). P-value *p* refers to the chi-squared test for the association between HRe and BO03/BO06 trial. Right panel: boxplots of final, pre-operative and post-operative Received Dose Intensity (i.e.,  $RDI_i$ ,  $RDI_{i,pre}$ ,  $RDI_{i,post}$ ) grouped by cohort (gray: *All*; red: *BO03*; purple: *BO06*). Squares and diamonds represent minimum and maximum values, respectively. P-values *p* refer to Mann-Whitney U tests for the distribution of RDI values in BO03 vs BO06 cohorts.

**Received Dose Intensity:** *final* RDI is defined as the ratio between standardized dose  $\Delta_i$  and standardized time  $\Gamma_i$ , as follows

$$RDI_i = \frac{\Delta_i}{\Gamma_i}. \quad (4)$$

In general,  $\Delta_i \leq 1$  and  $\Gamma_i \geq 1$  due to dose reductions and delays, respectively, and so  $RDI_i \leq 1$ .

Instead of considering the whole treatment from cycle 1 to 6, standardized dose, time and RDI could be computed for *pre-operative* and *post-operative* periods separately. Appendix C reports how definitions in (2), (3) and (4) can be adapted to consider *pre* and *post-operative* periods separately, i.e.,  $\Delta_{i,k}$ ,  $\Gamma_{i,k}$  and  $RDI_{i,k}$  with  $k \in \{pre, post\}$ . Note that  $RDI_i \neq RDI_{i,pre} + RDI_{i,post}$ .

Figure 4 reports a summary of treatment exposure characteristics for the whole cohort and for each trial. The percentages of patients with a *good* HRe after surgical resection were 34.1% in the whole cohort (94 patients out of 276), 32.5% in BO03 (37 out of 114) and 35.2% in BO06 (57 out of 162). Overall, median value of final RDI was 0.759 (IQR=[0.649; 0.857]), with minimum and maximum values of 0.376 and 1.121, respectively. Median percentages of pre-operative and post-operative RDI were 0.810 (IQR=[0.727; 0.901]) and 0.723 (IQR=[0.584; 0.870]), respectively, confirming that reductions and delays are usually allocated in the post-operative cycles.

Figure 5 shows a scatter plot of RDI at the end of treatment (final  $RDI_i$ ) against the final standardized dose of CDDP+DOX ( $\Delta_i$ ) for each trial (left panel: *BO03*; right panel: *BO06*) and HRe (blue: *poor*; green: *good*). The pink horizontal solid lines vertically divide patients with *normal* RDI levels ( $RDI_i \geq 0.85$ ) from *low* ( $0.70 \leq RDI_i < 0.85$ ) and *high* reduction ( $RDI_i < 0.70$ ) patients. The black diagonal solid line satisfies equation  $RDI_i = \Delta_i$ , dividing the group of patients with standardized time  $\Gamma_i > 1$  (delayed therapy, below the line) from the group of patients with  $\Gamma_i < 1$  (anticipated therapy, above the line). The black diagonal dotted line satisfies equation  $RDI_i = \Delta_i/1.2$ , dividing the group of patients with therapy delayed by more than 20% of anticipated time (below the dotted line) from the group of patients with therapy delayed by less than 20% of anticipated time (between solid and dotted black lines). This figure shows lack

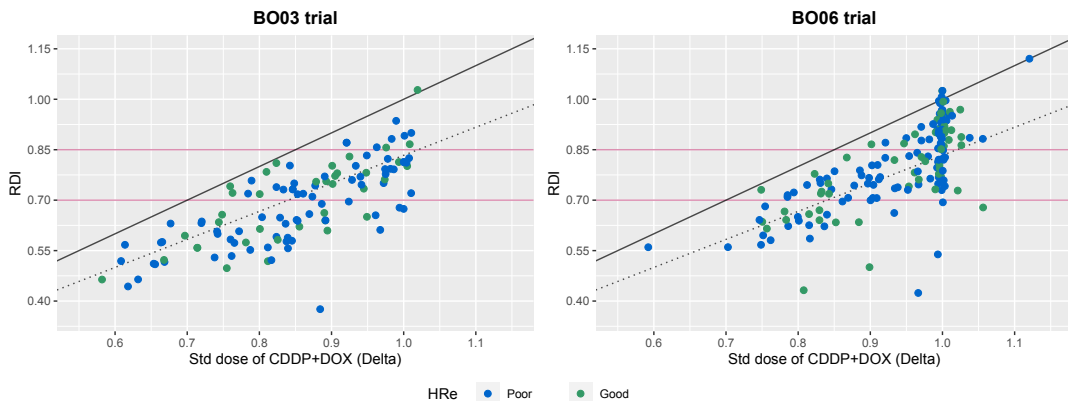


**Figure 5:** Scatter plots of RDI at the end of treatment (i.e.,  $RDI_i$  in Equation (4)) against the final standardized dose of CDDP+DOX ( $\Delta_i$ ) conditional on trial (*BO03*: left panel; *BO06*: right panel) and HRe (*poor*: blue points; *good*: green points).

of a clear association between HRe and RDI. Similar figures for pre/post-operative RDI against their relative standardized doses can be found in Appendix C. Both Figures 4 and 5 clearly display differences in treatment delivery for the BO03 and BO06 trials.

### 3 Causal inference structure and methods

Since negative feedback between therapy administration and toxicities acts as a (time-dependent) confounder for the effect of chemotherapy exposure on outcome, the novelty of this study is to create a pseudo-population in which medical history no longer predicts exposure through IPTW. Cox MSMs can be used to estimate the joint causal effect of HRe and dose intensity on Event-Free-Survival (EFS). In order to create such a pseudo-population, outcome, exposure, confounders and their mutual relationships have to be defined. EFS outcome is provided in Section 3.1. Causal inference assumptions for MSMs are introduced in Section 3.2. The causal structure of the chemotherapy data is given in Section 3.3. Two alternative definitions of joint-exposure with their relative models are finally introduced in Sections 3.4 and 3.5.

#### 3.1 Event-Free Survival Outcome

The endpoint of this study is EFS, defined as time from the end of therapy until the first event (local recurrence, evidence of new or progressive metastatic disease, second malignancy, death, or a combination of those events) or censoring at last contact.

**EFS outcome.** The time-to-event outcome for patient  $i \in \{1, \dots, N\}$  is denoted by  $(T_i, D_i)$ , where  $T_i = \min(T_i^*, C_i)$  is the observed EFS time,  $T_i^*$  is the true event time,  $C_i$  is the censoring time (i.e., the time from the end of the therapy until the last visit) and  $D_i = I(T_i^* \leq C_i)$  is the event indicator, with  $I(\cdot)$  being the indicator function that takes the value 1 when  $T_i^* \leq C_i$ , and 0 otherwise.

#### 3.2 Causal inference assumptions for marginal structural models

Marginal structural Cox models allow the estimation of the causal associations between treatment exposure  $\mathbf{A}$  and time-to-event response  $T$  in the presence of time-dependent covariates  $\mathbf{L}$  that may

be simultaneously confounders and intermediate variables.<sup>20,32,33</sup> Cox MSMs target *counterfactual* (or *potential*) time-to-event variables  $T^{\mathbf{a}}$ , i.e., the time at which an event would have been observed had the subject, possibly contrary to fact, been administered treatment exposure  $\mathbf{A} = \mathbf{a}$ . The main assumptions for causal inference with (Cox) MSMs through IPTW<sup>22,23</sup> are discussed.

### 1. *Exchangeability* or *No unmeasured confounding*

Exchangeability (or conditional exchangeability) implies the well-known assumption of *no unmeasured confounding*.<sup>23</sup> It states that exposure allocation is independent of the potential outcomes conditional on pre-treatment covariates (i.e.,  $T^{\mathbf{a}} \perp\!\!\!\perp \mathbf{A} | \mathbf{L}$ ) or, in a longitudinal setting, that treatment is sequentially randomized given the past.<sup>23</sup> This assumption is often referred as “ignorable treatment assignment” or “sequential randomization” in statistics, “selection on observables” in the social sciences or “no omitted variable bias” in econometrics.<sup>22</sup>

In absence of randomization, such as in observational studies, exchangeability cannot be tested. Experts knowledge is then necessary for the identification of enough joint predictors of exposure and outcome such that, within the levels of these predictors, associations between exposure and outcome that are due to their common causes are no longer present.<sup>23</sup>

### 2. *Consistency*

Consistency means that the outcome observed for each individual is the counterfactual outcome under the observed treatment history, that is  $T^{\mathbf{a}} = T$  for every individual with  $\mathbf{A} = \mathbf{a}$ . This assumption is violated in the presence of misclassification bias<sup>34</sup> and has two requirements:<sup>22</sup>

- i. the exposure must be *properly defined* so that the counterfactual outcomes are well-defined (this implies that a specific exposure may be hypothetically assigned to a subject exposed to a different level);
- ii. a *link* between counterfactuals and observed data is reasonable in the context under study (this means that the equality should be valid for at least some individuals).

Although consistency can not be empirically verified, it is assumed to be plausible in observational studies of medical treatments, since it may be possible to change an individual’s treatment status.<sup>35</sup>

### 3. *Positivity*

Positivity states that there is a non-zero (i.e., positive) probability of receiving every level of exposure for every combination of values of exposure and covariate histories that occur among individuals in the population.<sup>23</sup> If this assumption is violated, then the weights in IPTW are undefined leading to biased estimates of the causal effect.

If a subject cannot be exposed to one or more levels of the confounders (e.g., it cannot be treated in the presence of recommendations from guidelines or established contraindications), then positivity is violated due to a *structural zero* probability of receiving the specific exposure. A solution is to restrict the inference to the subset with a positive probability of exposure, whenever possible.<sup>35</sup> Even in the absence of structural zeros, *random zeros* may occur by chance due to small sample sizes or highly stratified data by numerous confounders. The inclusion of weak or highly-stratified confounders can provide a better confounding adjustment but may cause severe non-positivity, increasing the bias and variance of the estimated effect. An indication of non-positivity may be the presence of estimated weights with the mean far from one or very extreme values.<sup>35</sup>

#### 4. *No misspecification of both weighting and outcome models*

The final assumption of MSMs is that both the weighting model for IPTW and the structural outcome model, which links the outcome to the exposure history, must be correctly specified. This assumption has similar roots in all statistical models,<sup>34</sup> as model misspecification leads to instability in the Cox MSM estimates.<sup>33,36</sup>

Since the presence of estimated stabilized weights with the mean far from one or with extreme values suggest possible violation of positivity or misspecification of the weight model,<sup>35</sup> proper model specifications can be checked by exploring the distribution of weights.<sup>23</sup> In addition, quantitative (e.g., weighted standardized difference to compare means or prevalences) and qualitative graphical methods can be used to assess whether measured covariates are balanced between treatment groups in the weighted sample.<sup>37</sup>

If these assumptions hold, causal inference from MSMs through IPTW can be applied. In particular, IPTW creates a pseudo-population by weighting each patient with the inverse probability of observing a certain treatment allocation given the past treatment and confounders history. In the context of chemotherapy treatment, a pseudo-population created in this way has the following two properties:

- i. the past history of pseudo-patients no longer predicts exposure to chemotherapy in the next cycle;
- ii. the association between exposure and outcome is the same in both original and pseudo-population, so that causal effect of treatment modifications can be estimated by a crude analysis on the pseudo-population.

In the following sections, joint-exposure, confounders and Cox MSMs are introduced. Section 3.3 describes the causal structure of the chemotherapy data through the introduction of proper Direct Acyclic Graphs (DAGs) that identify all possible (time-dependent) confounders and their relationships with exposure and outcome. Once the appropriate DAGs according to clinical and statistical knowledge are constructed, it can be assumed that *exchangeability* is true within confounding strata. In Sections 3.4 and 3.5 two alternative definitions of exposure, which meet *consistency* according to experts' knowledge, are provided with relative counterfactual EFS outcomes and Cox MSMs. *Positivity* and *no misspecification* will be finally checked in Section 4.

### 3.3 Causal structure of chemotherapy data

Relationships between random variables (i.e., exposure, confounders and outcome) is usually represented using DAGs in causal inference.<sup>22,27</sup> Both clinical/oncological expertise in osteosarcoma treatment and statistical knowledge in variables definitions and mathematical modelling are required to construct a proper DAG for a specific context. Here the main interest is to estimate the joint causal effect of HRe and dose intensity reduction on EFS.

In both trials, HRe was defined after surgery and can be considered as a consequences of patient's pre-operative characteristics. Only the most severe CTCAE grades were recorded in BO03, while data from BO06 are fully longitudinal in both exposure and side-effects (see Section 2.2). This fact implies that therapy adjustment cannot be modelled cycle-by-cycle. Two novel methods are proposed for dose intensity:

1. *time-fixed final RDI*: the final value of RDI (i.e., the value at the end of treatment) can be seen as the result of the most severe toxicities experienced by the patient throughout the therapy;

2. *time-dependent pre/post-operative RDI*: therapy adjustment is modelled by pre/post-operative RDI, seen as the results of the most severe overall toxicities experienced by the patient during pre- or post-operative cycles.

The first option leads to a *time-fixed joint-exposure* of HRe and final RDI, whereas the second one to a *time-varying joint-exposure* given by HRe and time-varying pre/post-operative RDI.

Confounders were identified according to protocol guidelines and clinical knowledge. Conditioning chemotherapy administration over treatment as mentioned in Section 2.2, *rule-specific* and *generic* multiple overall toxicities represent time-dependent confounders. Influencing the drug metabolism, and so being risk factors for increased toxicity, age and gender are baseline confounders. Although the trial does not represent a proper risk factor for failures (p-value of log-rank test for Kaplan-Meier estimators stratified by trial is about 1), it can be considered as a baseline confounder, being both an independent predictor for HRe (through number of preoperative cycles<sup>26</sup> and therapy starting days) and for dose intensity (see Figures 3, 4, 5). In addition, HRe is associated to EFS through the way CTCAE grades were assessed and therapy modifications allocated (see Section 2.2). Furthermore, since there is a tendency not to delay surgery in the case of disease progression, the surgery timing may influence HRe.

Denote by  $\mathbf{L}_i$  and  $\mathbf{L}_{i,k}$  the vectors of *time-fixed* and *time-varying* confounders for patient  $i$  respectively, where  $k \in \{pre, post\}$  is the pre/post-operative index. Each vector component represents a variable influencing exposure and outcome. According to clinical knowledge, the following confounder vectors can be defined.

**Time-fixed confounders** for the  $i$ -th patient are represented by vectors of baseline and surgery characteristics, i.e.,  $\mathbf{L}_i^{base}$  and  $\mathbf{L}_i^{surg}$  with the following components:

- $L_i^{base,1}$ : trial number (BO03; BO06);
- $L_i^{base,2}$ : gender (*female*; *male*);
- $L_i^{base,3}$ : age group defined according to Collins *et al.* (2013)<sup>31</sup> (*child*: 0–12/0–11 years for males/females; *adolescent*: 13–17/12–16 years for males/females; *adult*: 18/17 or older for males/females);
- $L_i^{surg}$ : surgery time category with respect to schedule (0: *delayed*; 1: *on time* – see Table 1).

**Time-varying confounders** for the  $i$ -th patient are represented by the vectors of Multiple Overall Toxicity burden during pre/post-operative periods  $k \in \{pre, post\}$ , i.e.,  $\mathbf{L}_{i,pre}^{tox}$  and  $\mathbf{L}_{i,post}^{tox}$  with the following components:

- $L_{i,k}^{tox,1} = MOTox_{i,k}^{(rule)}$ : MOTox score related to period  $k$  based on *rule-specific* conditions  $\mathcal{M}^{(rule)}$ ;
- $L_{i,k}^{tox,2} = MOTox_{i,k}^{(gen)}$ : MOTox score related to period  $k$  based on *generic* conditions  $\mathcal{M}^{(gen)}$ .

The choice of MOTox scores, rather than individual CTCAE grades for the various toxicities, is motivated by the *positivity/confounders trade-off* and the clinical protocols. By considering the individual grades for each toxicity, the number of possible confounders combinations would be too high leading to non-positivity. This novel choice also meets the clinical rationale, in case of multiple toxicities, of adapting treatment according to the overall toxic burden of a patient (see Section 2.2).

According to experts knowledge, these characteristics satisfied the hypothesis of *no unmeasured confounding*. Baseline and pre-operative MOTox confounders affect both HRe and RDI. As delay in surgery time is already included in the calculation of the RDI, surgery only affects HRe (p-value of chi-squared test for association is 0.023). Being HRe the response to pre-operative treatment, post-operative MOTox confounders only influence RDI.

Figure 6 shows two novel DAGs resulting from the causal structure described above. DAG-1 (top panel) is characterized by EFS outcome, aforementioned confounders, and the time-fixed joint-exposure given by both HRe and final RDI. DAG-2 (bottom panel) identifies a relationship among EFS outcome, confounders and a time-varying joint-exposure given by HRe and pre/post-operative RDIs. Both DAGs rely upon the hypothesis that HRe and RDI(s) are conditionally independent on patient’s toxicity-history. Given two patients with the same toxicity history but different values of HRe, the probability of observing a reduction in RDI is the same in the two patients. This assumption is motivated by the following :

- i. HRe is not known until several weeks since chemotherapy is resumed after surgery, i.e., HRe could influence the decision to reduce therapy intensity only in the very last cycles;
- ii. few protocol violations are expected in a randomized clinical trial.

Moreover, both choices do not allow to use RDI as continuous variable, as this would not guarantee *consistency* and *positivity*. Therefore, a well-defined categorization of RDI exposure according to a clinical rational must be introduced.

### 3.4 Time-fixed joint-exposure and marginal structural Cox model for DAG-1

DAG-1 (top panel in Figure 6) is characterized by the EFS outcome  $T_i$ , the time-fixed and time-varying confounders  $(\mathbf{L}_i^{base}, L_i^{surg}, \mathbf{L}_{i,pre}^{tox}, \mathbf{L}_{i,post}^{tox})$ , and a joint-exposure  $\mathbf{A}_i$  given by HRe and final RDI, both time-fixed. According to expert knowledge, a *normal* RDI level (i.e.,  $RDI_i \geq 0.85$ ) can be analysed in contrast to *low* (from 15% to 30%) and *high* (more than 30%) reduction categories.

**Time-fixed joint-exposure.** The *time-fixed joint-exposure* administered for subject  $i$  is denoted by the vector

$$\mathbf{A}_i = (A_i^1, A_i^2) \tag{5}$$

where

- $A_i^1$  represents the three-level exposure related to final RDI

$$A_i^1 = \begin{cases} 0 & \text{if } RDI_i \geq 0.85 \\ 1 & \text{if } 0.70 \leq RDI_i < 0.85 \\ 2 & \text{if } RDI_i < 0.70 \end{cases}$$

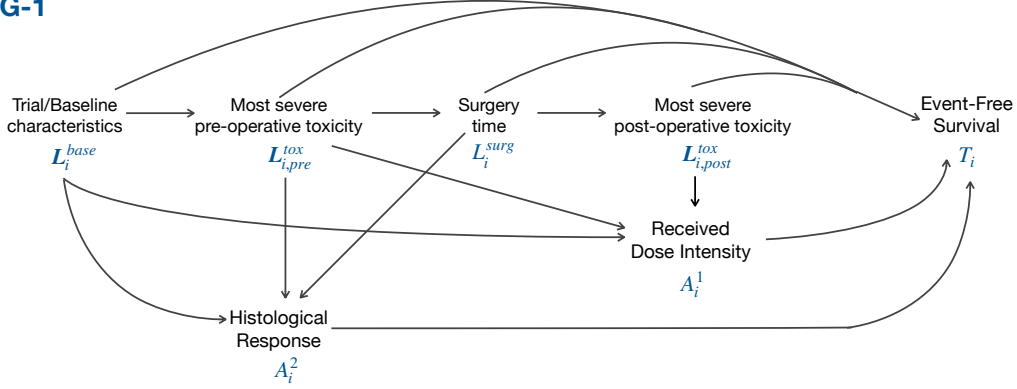
that is,  $A_i^1 = 0$  is equivalent to a “*normal*” RDI level,  $A_i^1 = 1$  to a “*low-reduction*” and  $A_i^1 = 2$  to a “*high-reduction*”;

- $A_i^2$  is the binary exposure related to HRe

$$A_i^2 = \begin{cases} 0 & \text{if tumour necrosis}_i < 90\% \\ 1 & \text{if tumour necrosis}_i \geq 90\% \end{cases}$$

that is,  $A_i^2 = 1$  is equivalent to a “*good*” HRe, while  $A_i^2 = 0$  denotes a “*poor*” HRe.

### DAG-1



### DAG-2

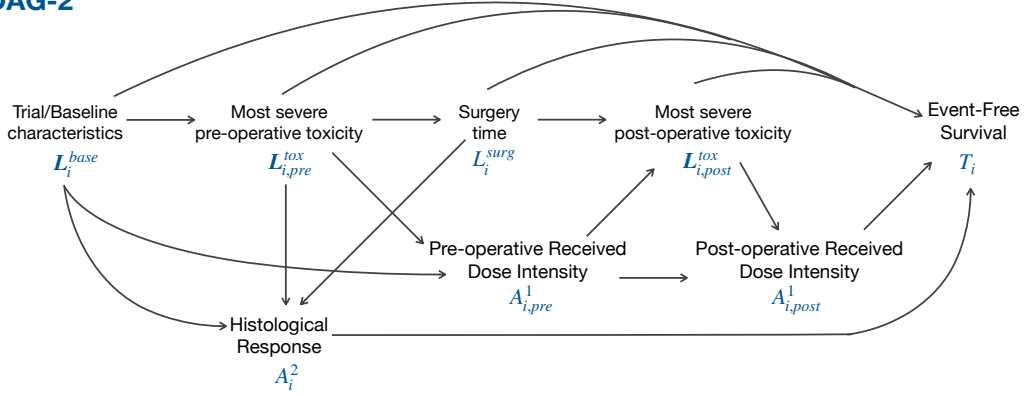


**Figure 6:** Directed Acyclic Graphs (DAGs) used to represent the causal relationships between event free survival outcome  $T_i$ , joint-exposure  $A_i$ , time-fixed confounders  $L_i$  (baseline and surgery) and time-varying confounders  $L_{i,k}$  (pre/post-operative multiple overall toxicities).  
Top panel (DAG-1): joint exposure is characterized by HRe and time-fixed final RDI.  
Bottom panel (DAG-2): joint-exposure is characterized by HRe and time-varying pre/post-operative RDI.

Once joint-exposure is properly defined, the counterfactual EFS outcome, i.e., the outcome that would be observed had the subject followed – possibly contrary-to-fact – a given treatment, is also well-defined.

**Counterfactual outcome.** Let  $T_i^a = T_i^{(a_1, a_2)}$  denote the counterfactual EFS time that would be observed in a subject  $i$  with joint-exposure treatment

$$A_i^1 = a_1, \quad a_1 \in \{0, 1, 2\}, \quad \text{and} \quad A_i^2 = a_2, \quad a_2 \in \{0, 1\}.$$

In particular, there are six joint-exposure  $(a_1, a_2)$  that can be realised according to (5):

- (0,0): *poor* responder without significant reduction (i.e., *normal* RDI level);
- (1,0): *poor* responder with final *low-reduction* of 15-30%;

- (2,0): *poor* responder with final *high-reduction* of more than 30%;
- (0,1): *good* responder without significant reduction;
- (1,1): *good* responder with final *low-reduction* of 15-30%;
- (2,1): *good* responder with final *high-reduction* of 30%.

Within a counterfactual framework, i.e., in the pseudo-population, Cox MSMs enable the conceptual comparison of the hazard functions for different treatment level  $\mathbf{a} = (a_1, a_2)$ . No baseline/-experimental covariates are included in the model because there is no clinical interest in assessing the causal effect of changes in chemotherapy exposure within specific population strata. The major interest consists in estimating a Cox MSM for the causal effect of RDI on EFS analogous to the Intention-To-Treat (ITT) Cox model presented by Lewis *et al.* (2007).<sup>26</sup> The latter model included HRe, intended treatment, and their interaction. A Cox MSM with interaction between  $a_1$  and  $a_2$ , where the treatment binary variable is replaced by the actual final RDI level, is hence proposed here.

**Cox MSM 1** for EFS time under treatment level  $\mathbf{a} = (a_1, a_2)$ :

$$h_{T_i^{\mathbf{a}}}(t) = h_0(t) \exp \left\{ \beta_1 \mathbb{1}_{(a_1=1)} + \beta_2 \mathbb{1}_{(a_1=2)} + \beta_3 a_2 + \beta_4 \mathbb{1}_{(a_1=1)} a_2 + \beta_5 \mathbb{1}_{(a_1=2)} a_2 \right\}. \quad (6)$$

To estimate the causal parameters  $\beta$  of the Cox MSM in Equation (6), a weighted Cox model<sup>38,39</sup> can be fitted to the pseudo-population obtained through IPTW, as follows

$$h_{T_i}^{SW_i}(t|\mathbf{A}_i) = h_0(t) \exp \left\{ \theta_1 \mathbb{1}_{(A_i^1=1)} + \theta_2 \mathbb{1}_{(A_i^1=2)} + \theta_3 A_i^2 + \theta_4 \mathbb{1}_{(A_i^1=1)} A_i^2 + \theta_5 \mathbb{1}_{(A_i^1=2)} A_i^2 \right\} \quad (7)$$

with subject-specific stabilized weights

$$SW_i = SW_i^{A^1} \cdot SW_i^{A^2} \quad (8)$$

where

$$SW_i^{A^1} = \frac{P(A_i^1)}{P(A_i^1 | \mathbf{L}_i^1)} = \frac{P(A_i^1)}{P(A_i^1 | \mathbf{L}_i^{base}, \mathbf{L}_{i,pre}^{tox}, \mathbf{L}_{i,post}^{tox})};$$

$$SW_i^{A^2} = \frac{P(A_i^2)}{P(A_i^2 | \mathbf{L}_i^2)} = \frac{P(A_i^2)}{P(A_i^2 | \mathbf{L}_i^{base}, \mathbf{L}_{i,pre}^{tox}, L_i^{surg})}.$$

In both  $SW_i^{A^1}$  and  $SW_i^{A^2}$ , numerators are the probability that a subject  $i$  received exposures  $A_i^1$  and  $A_i^2$  respectively, whereas denominators are the probability that the subject received exposures given relative time-fixed and time-dependent confounders. Regression models have to be chosen according to the type of exposure. In particular, multinomial logistic regression models are used for both numerator and denominator of  $SW_i^{A^1}$ , whereas binary logistic regression models are adopted for  $SW_i^{A^2}$ .

Under causal inference assumptions (see Section 3.2), association is causation in the pseudo-population and the estimates of the associational parameters  $\theta$  are consistent for the causal parameters  $\beta$ . A note of caution is required in applying this methodology to the chemotherapy data. Different model specifications in terms of confounding covariate features must be compared to satisfy the final assumptions of *positivity* and *no misspecification of the weight-generating models* and guarantee an unbiased estimation of the results.

### 3.5 Time-varying joint-exposure and marginal structural Cox model for DAG-2

DAG-2 (bottom panel in Figure 6) is characterized by the EFS outcome  $T_i$ , time-fixed and time-varying confounders  $(\mathbf{L}_i^{base}, L_i^{surg}, \mathbf{L}_{i,pre}^{tox}, \mathbf{L}_{i,post}^{tox})$ , and a joint-exposure  $\bar{\mathbf{A}}_i$  given by HRe and time-varying pre/post-operative RDI. As in the previous section, a *normal* RDI level can be analysed in contrast to *low* and *high* reductions. Time-varying joint-exposure  $\bar{\mathbf{A}}_i$  for DAG-2 is hence defined as follows.

**Time-varying joint-exposure.** The *time-varying joint-exposure* administered to subject  $i$  is denoted by the vector

$$\bar{\mathbf{A}}_i = (\bar{\mathbf{A}}_i^1, A_i^2) = ((A_{i,pre}^1, A_{i,post}^1), A_i^2) \quad (9)$$

where

- $\bar{\mathbf{A}}_i^1$  represents the time-varying three-level exposure vector related to pre/post-operative RDI with elements

$$A_{i,k}^1 = \begin{cases} 0 & \text{if } RDI_{i,k} \geq 0.85 \\ 1 & \text{if } 0.70 \leq RDI_{i,k} < 0.85 \\ 2 & \text{if } RDI_{i,k} < 0.70 \end{cases}$$

that is,  $A_{i,k}^1 = 0$  is equivalent to a “*normal*” RDI level,  $A_{i,k}^1 = 1$  to a “*low-reduction*” and  $A_{i,k}^1 = 2$  to a “*high-reduction*” and  $k \in \{pre, post\}$  indicates the *pre-operative* and *post-operative* periods, respectively;

- $A_i^2$  is the binary exposure related to HRe

$$A_i^2 = \begin{cases} 0 & \text{if tumour necrosis}_i < 90\% \\ 1 & \text{if tumour necrosis}_i \geq 90\% \end{cases}$$

that is,  $A_i^2 = 1$  is equivalent to a “*good*” HRe, while  $A_i^2 = 0$  denotes a “*poor*” HRe.

Once joint-exposure is properly defined, the counterfactual EFS outcome, i.e., the outcome that would be observed had the subject followed – possibly contrary-to-fact – a given treatment, is also well-defined.

**Counterfactual outcome.** Let  $T_i^{\bar{\mathbf{a}}} = T_i^{((a_{11}, a_{12}), a_2)}$  denote the counterfactual EFS time that would be observed in a subject  $i$  with time-varying joint-exposure

$$A_{i,pre}^1 = a_{11}, \quad A_{i,post}^1 = a_{12}, \quad a_{11}, a_{12} \in \{0, 1, 2\}, \quad \text{and} \quad A_i^2 = a_2, \quad a_2 \in \{0, 1\}.$$

In particular, there are 18 time-varying joint-exposure combinations  $\bar{\mathbf{a}} = (\bar{\mathbf{a}}_1, a_2) = ((a_{11}, a_{12}), a_2)$  that can be realised according to (9). To avoid too many combinations, we specify a model that combines information from many strategies to guarantee *positivity* and help estimate the causal effects. Define the cumulative treatment effects under sub-strategy  $\bar{\mathbf{a}}_1$ , named *cumulative RDI-exposure*, as follows

$$\text{cum}(\bar{\mathbf{a}}_1) = \sum_{k=1}^2 a_{1k}$$

which could takes value

- 0: no reduction;

- 1: only one *low* reduction pre or post surgery;
- 2: *low* reductions both pre and post surgery or *high* reduction pre or post surgery;
- 3: both pre-operative (post-operative) *low* reduction and post-operative (pre-operative) *high* reduction;
- 4: *high* reductions pre and post surgery.

Therefore  $\text{cum}(\bar{a}_1)$  represents the number of reductions by a value of 15-30%. A single *high* reduction of at least 30% can be seen as twice a *low* reduction of 15-30%. In the following, the *time-varying joint-exposure* levels and values for patient  $i$  (with 18 different possible combinations) are indicated by  $\bar{a} = (\bar{a}_1, a_2)$  and  $\bar{A}_i = (\bar{A}_i^1, A_i^2)$  respectively. The *cumulative joint-exposure* levels and values for patient  $i$  (with 10 different possible combinations) are indicated by  $\tilde{a} = (\text{cum}(\bar{a}_1), a_2)$  and  $\tilde{A}_i = (\text{cum}(\bar{A}_i^1), A_i^2)$ , respectively.

Within a counterfactual framework, Cox MSMs enable the conceptual comparison of the hazard functions for different treatment exposure  $\bar{a} = (\bar{a}_1, a_2)$ . As in Section 3.4, no baseline/trial covariates are included in this structural model. Since the interests is in analysing the causal RDI analogue of the ITT Cox model presented by Lewis *et al.* (2007)<sup>26</sup> according to pre/post-operative RDI definitions, a Cox MSM with interaction between  $\text{cum}(\bar{a}_1)$  and  $a_2$  is proposed.

**Cox MSM 2** for EFS time under cumulative treatment level  $\tilde{a} = (\text{cum}(\bar{a}_1), a_2)$ :

$$h_{T_i^{\tilde{a}}}(t) = h_0(t) \exp \{ \beta_1 \text{cum}(\bar{a}_1) + \beta_2 a_2 + \beta_3 \text{cum}(\bar{a}_1) a_2 \} \quad (10)$$

To estimate the causal parameters  $\beta$  of the Cox MSM in Equation (10), a weighted Cox model<sup>38,39</sup> can be fitted to the pseudo-population obtained through IPTW, as follows

$$h_{T_i}^{SW_i}(t|\bar{A}_i) = h_0(t) \exp \{ \theta_1 \text{cum}(\bar{A}_i^1) + \theta_2 A_i^2 + \theta_3 \text{cum}(\bar{A}_i^1) A_i^2 \} \quad (11)$$

where  $\text{cum}(\bar{A}_i^1)$  is the cumulative RDI-exposure vector

$$\text{cum}(\bar{A}_i^1) = \sum_{k \in \{pre, post\}} A_{i,k}^1$$

and  $SW_i$  are the subject-specific stabilized weights given by

$$SW_i = SW_i^{\bar{A}^1} \cdot SW_i^{A^2} = \left( SW_i^{A_{pre}^1} \cdot SW_i^{A_{post}^1} \right) \cdot SW_i^{A^2} \quad (12)$$

with

$$\begin{aligned} SW_i^{A_{pre}^1} &= \frac{P(A_{i,pre}^1)}{P(A_{i,pre}^1 | \mathbf{L}_{i,pre}^1)} = \frac{P(A_{i,pre}^1)}{P(A_{i,pre}^1 | \mathbf{L}_i^{base}, \mathbf{L}_{i,pre}^{tox})}; \\ SW_i^{A_{post}^1} &= \frac{P(A_{i,post}^1 | A_{i,pre}^1)}{P(A_{i,post}^1 | A_{i,pre}^1, \bar{\mathbf{L}}_{i,post}^1)} = \frac{P(A_{i,post}^1 | A_{i,pre}^1)}{P(A_{i,post}^1 | A_{i,pre}^1, \mathbf{L}_i^{base}, \mathbf{L}_{i,pre}^{tox}, \mathbf{L}_{i,post}^{tox})}; \\ SW_i^{A^2} &= \frac{P(A_i^2)}{P(A_i^2 | \mathbf{L}_i^2)} = \frac{P(A_i^2)}{P(A_i^2 | \mathbf{L}_i^{base}, \mathbf{L}_{i,pre}^{tox}, L_i^{surg})}. \end{aligned}$$

Particular attention for *positivity* and *no misspecification of the weight-generating models* is required also in this context. Multinomial logistic regression models can be used for both numerators and denominators of  $SW_i^{A^1_{pre}}$  and  $SW_i^{A^1_{post}}$ , whereas binary logistic regression models can be adopted for  $SW_i^{A^2}$ . Under causal inference assumptions, association is causation in the pseudo-population, i.e.,  $\theta$  is consistent with  $\beta$ .

## 4 Results

IPTW-based causal methodologies introduced in Section 3 are now applied to BO03-BO06 chemotherapy data presented in Section 2. In Section 4.1 joint-exposures for DAG-1 and DAG-2 are explored in terms of percentages of patients in each exposure-level and association with EFS in the original population. Different IPTW model specifications to determine the subject-specific standardized weights for the pseudo-population are presented in Section 4.2. Results based on the causal Cox MSMs fitted on the pseudo-population are presented in Section 4.3, along with the unweighted Cox results to show the *toxicity-treatment-adjustment* bias present in the original data.

Statistical analyses were performed in the R-software environment,<sup>40</sup> in particular using `ipw`<sup>41</sup> and `survival`<sup>42</sup> packages.

### 4.1 Joint-exposure descriptive and association with EFS

Median EFS time computed using the reverse Kaplan-Meier method by Schemper and Smith (1996)<sup>43</sup> was 89.59 months (IQR = [50.33; 146.30]) and 155 patients (55.1%) experienced an event after the end of the therapy. Figure 7 shows *time-fixed*  $A_i$  (top panels) and *cumulative*  $\tilde{A}_i$  (bottom panels) joint-exposure characteristics. Left panels report percentage of patients according to the various joint-exposure levels and right panels display Kaplan-Meier estimators for EFS curves stratified by joint-exposure levels with time in months since end of therapy. *Good* Responders (GRs) showed a better survival with respect to *Poor* ones (PRs). In GRs an increased final/cumulative RDI seemed associated with better survival, whereas a reversed association was observed in the group of PRs. In both cases the estimated survival for GRs with the highest reduction and for PRs were very similar. This validated the inclusion of the interaction term between the joint-exposure components in Cox MSMs (6) and (10).

To further investigate these findings and analyse the causal effect of time-fixed/time-varying joint-exposure on EFS through Cox MSMs, subject-specific standardized weights must be computed from correctly specified IPTW models which take into account all the confounding factors identified in Section 3.3.

### 4.2 IPTW diagnostics

Different specifications of the subject-specific standardized weights for final RDI level  $SW_i^{A^1}$ , HR category  $SW_i^{A^2}$  and pre/post-operative RDI levels  $SW_i^{\tilde{A}^1} = SW_i^{A^1_{pre}} \cdot SW_i^{A^1_{post}}$  were investigated in order to check whether and which models best satisfied *positivity* and *no misspecification*. As discussed in Sections 3.4 and 3.5, multinomial logistic regression models were used for both numerators and denominators of  $SW_i^{A^1}$  and  $SW_i^{\tilde{A}^1}$ , whereas binary logistic regression models were adopted for  $SW_i^{A^2}$ . In all cases, the following four different model specifications in terms of confounding features for the denominators were compared.

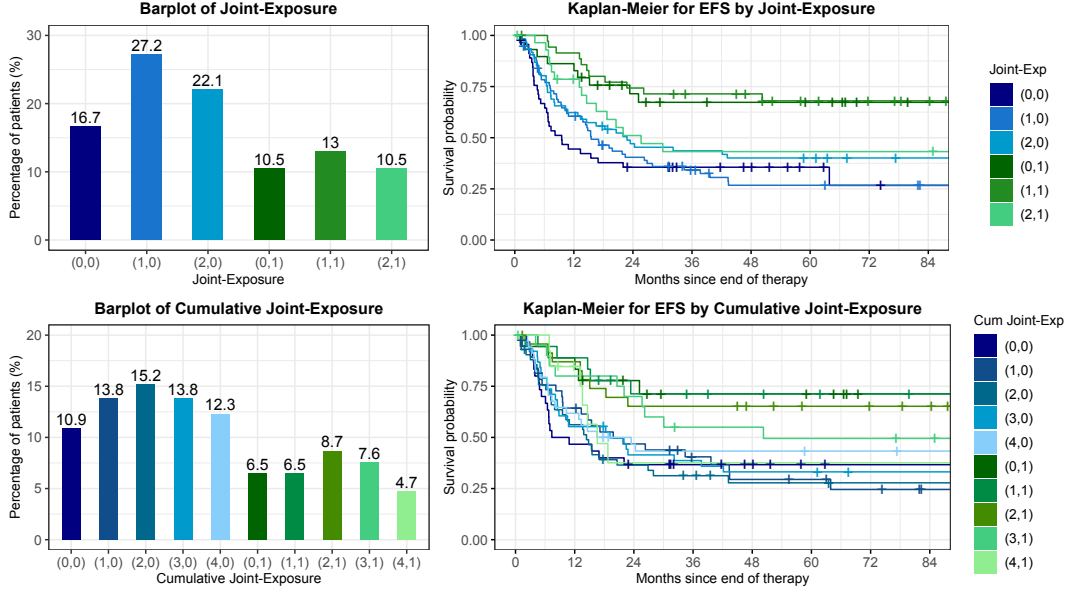


**Figure 7:** Joint-exposure characteristics.

Top panels: *time-fixed joint-exposure*  $A_i = (A_i^1, A_i^2)$  defined in Section 3.4. Final RDI level is  $A_i^1$  with levels  $\in \{0: \text{normal } RDI_i \geq 0.85; 1: \text{low-reduction } 0.70 \leq RDI_i < 0.85; 2: \text{high-reduction } RDI_i < 0.70\}$ . HRe is  $A_i^2$  with categories  $\in \{0: \text{poor}; 1: \text{good}\}$ .

Bottom panels: *cumulative joint-exposure*  $\tilde{A}_i = (\text{cum}(\tilde{A}_i^1), A_i^2)$ . Cumulative pre/post-operative RDI level is  $\text{cum}(\tilde{A}_i^1)$  with values  $\in \{0: \text{no reduction}; 1: \text{only one low reduction pre or post surgery}; 2: \text{low reductions both pre and post surgery or high reduction pre or post surgery}; 3: \text{one low reduction and one high reduction}; 4: \text{high reductions pre and post surgery}\}$ . HRe is  $A_i^2$  with categories  $\in \{0: \text{poor}; 1: \text{good}\}$ . Left panels: percentage of patients by joint-exposure levels. Right panels: Kaplan-Meier estimators for EFS stratified by joint-exposure levels.

**IPTW 1:** Each confounding covariate was included in the models as a main effect only and the MOTox scores were linearly related to the log-odds. The vectors of confounding covariates for each denominator model were defined as follows:

$$\begin{aligned}
SW_i^{A^1} : L_i^1 &= \left( L_i^{base}, L_{i,pre}^{tox}, L_{i,post}^{tox} \right) \\
&= \left( \text{trial}_i, \text{age}_i, \text{gender}_i, \text{MOTox}_{i,pre}^{(gen)}, \text{MOTox}_{i,pre}^{(rule)}, \text{MOTox}_{i,post}^{(gen)}, \text{MOTox}_{i,post}^{(rule)} \right); \\
SW_i^{A^2} : L_i^2 &= \left( L_i^{base}, L_{i,pre}^{tox}, L_i^{surg} \right) \\
&= \left( \text{trial}_i, \text{age}_i, \text{gender}_i, \text{MOTox}_{i,pre}^{(gen)}, \text{MOTox}_{i,pre}^{(rule)}, \text{surgery}_i \right); \\
SW_i^{A_{pre}^1} : L_{i,pre}^1 &= \left( L_i^{base}, L_{i,pre}^{tox} \right) \\
&= \left( \text{trial}_i, \text{age}_i, \text{gender}_i, \text{MOTox}_{i,pre}^{(gen)}, \text{MOTox}_{i,pre}^{(rule)} \right); \\
SW_i^{A_{post}^1} : \bar{L}_{i,post}^1 &= \left( L_i^{base}, L_{i,pre}^{tox}, L_{i,post}^{tox} \right) \\
&= \left( \text{trial}_i, \text{age}_i, \text{gender}_i, \text{MOTox}_{i,pre}^{(gen)}, \text{MOTox}_{i,pre}^{(rule)}, \text{MOTox}_{i,post}^{(gen)}, \text{MOTox}_{i,post}^{(rule)} \right).
\end{aligned}$$

**Table 2:** Inverse Probability of Treatment Weighting (IPTW) diagnostics based on summaries of stabilized weights related to final RDI level  $SW_i^{A^1}$ , HRe category  $SW_i^{A^2}$  and pre/post-operative RDI levels  $SW_i^{\bar{A}^1}$  computed using the four different specifications listed in Section 4.2.

Final RDI level: $SW_i^{A^1}$		
Specification	Mean (s.d.)	Min/Max
IPTW 1	0.988 (0.668)	0.330/5.252
IPTW 2	0.987 (0.682)	0.354/5.189
IPTW 3	0.979 (0.700)	0.324/5.469
IPTW 4	0.968 (0.797)	0.326/6.946
HRe: $SW_i^{A^2}$		
Specification	Mean (s.d.)	Min/Max
IPTW 1	1.001 (0.200)	0.598/1.746
IPTW 2	1.001 (0.201)	0.603/1.780
IPTW 3	1.001 (0.242)	0.578/2.116
IPTW 4	0.999 (0.250)	0.531/2.373
Pre/Post RDI levels: $SW_i^{\bar{A}^1}$		
Specification	Mean (s.d.)	Min/Max
IPTW 1	0.988 (0.839)	0.285/7.109
IPTW 2	0.994 (0.910)	0.267/8.555
IPTW 3	0.998 (1.101)	0.266/11.438
IPTW 4	0.998 (1.245)	0.161/12.959

**IPTW 2:** Same covariates as in IPTW 1 + interaction terms for toxicity confounders linearly related to the log-odds:

- (i) interaction between pre-operative rule-specific and generic MOTox scores:  $\text{MOTox}_{i,pre}^{(gen)} \cdot \text{MOTox}_{i,pre}^{(rule)}$ ;
- (ii) interaction between post-operative rule-specific and generic MOTox scores:  $\text{MOTox}_{i,post}^{(gen)} \cdot \text{MOTox}_{i,post}^{(rule)}$  (only for final and post-operative RDI).

**IPTW 3:** Same covariates as in IPTW 1 + interaction terms between toxicities and trial linearly related to the log-odds:

- (i) two interactions between pre-operative MOTox score and trial:  $\text{MOTox}_{i,pre}^{(m)} \cdot \text{trial}_i$ ,  $m \in \{gen, rule\}$ ;
- (ii) two interactions between post-operative MOTox score and trial:  $\text{MOTox}_{i,post}^{(m)} \cdot \text{trial}_i$ ,  $m \in \{gen, rule\}$  (only for final and post-operative RDI).

**IPTW 4:** Each categorical/binary confounding covariates (i.e.,  $\text{trial}_i$ ,  $\text{age}_i$ ,  $\text{gender}_i$ ,  $\text{surgery}_i$ ) was included in the models as a main effect only. B-spline basis matrix for cubic polynomial splines with three internal knots were used to model the relationship between each continuous MOTox score and the log-odds:  $\mathbf{B}(\text{MOTox}_{i,k}^{(m)}) \forall m \in \{gen, rule\}, k \in \{pre, post\}$ .

Table 2 reports the summaries of the stabilized weights obtained with different specifications for final RDI level  $SW_i^{A^1}$ , HRe category  $SW_i^{A^2}$  and pre/post-operative RDI levels  $SW_i^{\bar{A}^1}$ .

By examining the distributions of the standardized weights for final RDI, there was no evidence of violation of the positivity or misspecification assumptions for IPTW methods 1 and 2 (mean values of about 0.99 without extreme values), whereas methods 3 and 4 presented lower mean

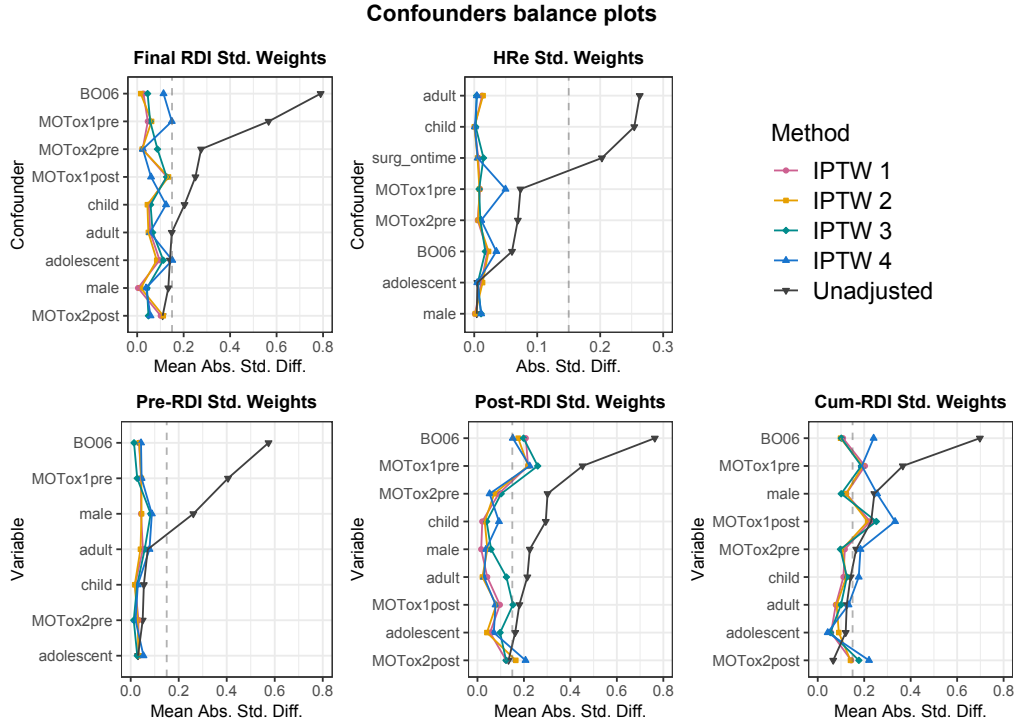


**Figure 8:** Diagnostic balance plot for Inverse Probability of Treatment Weighting (IPTW). Lines represent the (mean) absolute standardized differences for each exposure-related confounder according to the four different specification methods introduced in Section 4.2 and their unadjusted versions (pink: *IPTW 1*; orange: *IPTW 2*; green: *IPTW 3*; blue: *IPTW 4*; black: *Unadjusted*).

values and higher standard deviations. The same was confirmed by the diagnostics balance plot in top-left panel of Figure 8. The mean absolute standardized differences for final RDI confounders in the unweighted sample (black points) always exceeded those in the weighted samples, and the lowest values were observed for IPTW 1 and 2. IPTW model 1 was finally selected among the two as it had a mean value closer to 1 and lower standard deviation.

Similarly, according to the distributions of the standardized weights for HRe models, there was no evidence of non-positivity or misspecification in the four IPTW methods: they all presented a mean value of 1 with standard deviation from 0.22 to 0.25. In terms of covariates balance (top-right panel in Figure 8), all IPTW methods performed better than the unweighted sample (black) but IPTW 4 (blue) was worse than the others. IPTW model 1 was finally selected as it was simpler and had lower standard deviation weights.

IPTW methods for pre/post-operative RDI levels was selected according to the distributions of the standardized weights  $SW_i^{\bar{A}^1}$ , as trade-off between the two product components. IPTW 4 method resulted in a worse balance of confounders in terms of mean absolute standardised differences for cumulative-RDI levels based on  $SW_i^{\bar{A}^1}$  (bottom-right panel in Figure 8). The same was valid for post-RDI levels using  $SW_i^{A^1_{post}}$  obtained through IPTW 3 (bottom-centre panel). Between IPTW methods 1 and 2, both with a mean value of about 0.99, IPTW 1 was selected as it was simpler and had lower standard deviation weights.

The denominators of  $SW_i^{A^1}$ ,  $SW_i^{A^1_{pre}}$ ,  $SW_i^{A^1_{post}}$  and  $SW_i^{A^2}$  related to the selected IPTW spec-

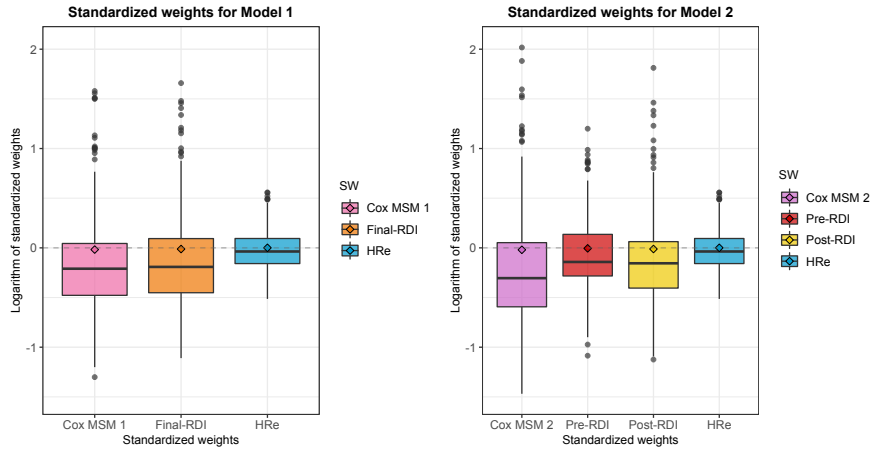


**Figure 9:** Diagnostic boxplots of subject-specific standardized weights computed via Equations (8) (left panel) and (12) (right panel). The scale on the y-axis is logarithmic. Diamonds represent the mean values (in logarithmic scale).

ifications are reported in Appendix D.

Left panel of Figure 9 shows the standardized weights  $SW_i$  in (8) obtained as product of  $SW_i^{A^1}$  and  $SW_i^{A^2}$  to be used to create the pseudo-population in case of *time-fixed joint exposure*. The y-axis is in logarithmic scale. Mean value of  $SW_i$  was 0.983 ( $s.d. = 0.694$ ) with minimum and maximum values of 0.272 and 4.849. Analogously, right panel of Figure 9 shows the standardized weights  $SW_i$  in (12) obtained as product of  $SW_i^{A^1}$  and  $SW_i^{A^2}$  to be used to create the pseudo-population in case of *time-varying joint exposure*. Mean value of  $SW_i$  was 0.981 ( $s.d. = 0.865$ ) with minimum and maximum values of 0.230 and 7.518. These weights satisfied all the required assumptions and were finally used to fit on the relative pseudo-populations the IPT weighted Cox models in (7) and (11).

### 4.3 Causal inference through marginal structural Cox models

The causal parameters  $\beta$  in Cox MSMs (6) and (10) were hence estimated through their consistent parameters  $\theta$  in weighted Cox models (7) and (11) fitted on the relative pseudo-populations. Estimates were finally compared to the results obtained by fitting the traditional Cox models on the original population.

Estimated parameters for both Cox MSMs and their unweighted versions are reported in Table 3. In Cox MSM 1 and 2 robust standard errors for computing the confidence interval of each coefficient were obtained via the option `robust=TRUE` in R function `coxph`.<sup>42</sup> Figure 10 displays the Hazard Ratios related to the different joint-exposure levels for Cox MSMs in (6) and (10) fitted on the pseudo population (left panels) and the results for corresponding unweighted models (right panels).

Top panels in Figure 10 refers to the causal structure of DAG-1 presented in Section 3.4. Reference level was PRs with *normal* RDI level at the end of treatment, i.e.,  $(a_1, a_2) = (0, 0)$ . Considering the unweighted Cox model 1 (top-right), which represents the RDI-analogue of the ITT Cox model presented by Lewis *et al.* (2007)<sup>26</sup> without considering IPT weights, in PRs the RDI reductions seemed associated with an improvement in EFS, even if not statistically significant. GRs receiving a *normal* RDI compared to GRs receiving a *low-reduction* experienced an event 12% slower ( $HR = 0.273/0.309 = 0.88$ ) whereas those receiving a *high-reduction* experienced an event

**Table 3:** Estimated parameters  $\hat{\beta}$  along with their 95% Confidence Intervals (CIs) for Cox MSMs 1 and 2 in Equation ((6)) and ((10)), respectively, and for their corresponding unweighted versions.

Treatment	Cox MSM 1		Unweighted Cox model 1	
	$\hat{\beta}$	95% CIs	$\hat{\beta}$	95% CIs
$a_1 = 1$	-0.498	[-0.986; -0.010]	-0.116	[-0.568; 0.335]
$a_1 = 2$	-0.833	[-1.409; -0.257]	-0.359	[-0.844; 0.127]
$a_2 = 1$	-1.914	[-2.880; -0.948]	-1.175	[-1.921; -0.429]
$a_1 = 1 \times a_2 = 1$	0.762	[-0.399; 1.923]	-0.006	[-0.997; 0.984]
$a_1 = 2 \times a_2 = 1$	1.850	[0.643; 3.057]	0.979	[0.020; 1.938]
Treatment	Cox MSM 2		Unweighted Cox model 2	
	$\hat{\beta}$	95% CIs	$\hat{\beta}$	95% CIs
cum( $\bar{a}_1$ )	-0.181	[-0.370; 0.009]	-0.062	[-0.197; 0.072]
$a_2 = 1$	-1.823	[-2.714; -0.932]	-1.461	[-2.215; -0.707]
cum( $\bar{a}_1$ ) $\times$ $a_2 = 1$	0.397	[0.052; 0.743]	0.305	[0.010; 0.601]

86% faster ( $HR = 0.574/0.309 = 1.86$ ). However, these results were affected by the toxicity-treatment-adjustment bias and could not be interpreted in a causal way. The final value of RDI was the realisation of the treatment trajectory as result of both severity of the overall toxicity experienced by each patient and physicians' interventions. To overcome these issues, Cox MSM 1 (top-left) showed a clear improvement with respect to its unweighted version. At the same final RDI level, a *good* response caused an 85.2% decrease in the risk of an event ( $\exp(\hat{\beta}_3) = 0.148$ ) respect to a *poor* responder. Reductions in the final RDI caused better EFS for PRs, whereas a reverse causal association was founded in GRs. In particular, the higher the final reduction, the better the survival for PRs (estimated HRs were 0.608 and 0.435 for *low* and *high* reduction PRs, respectively). On the contrary, the higher the final reduction, the worsen the survival for GRs: GRs with *low* or *high* reduction experienced an event 1.30 ( $HR = 0.192/0.148 = 1.30$ ) or 2.76 ( $HR = 0.408/0.148 = 2.76$ ) times faster than GRs with *normal*-RDI.

Bottom panels in Figure 10 refers to the causal structure of DAG-2 presented in Section 3.5. Reference level was PRs without reduction, neither pre nor post surgery, i.e.,  $(\text{cum}(\bar{a}_1), a_2) = (0, 0)$ . Results were in line with previous results: (i) GRs presented better survival with respect to PRs; (ii) an increasing number of pre/post-operative reductions in RDI showed opposite trends for PRs and GRs, improving and worsening EFS, respectively. This was even more evident in the result of Cox MSM 2 (bottom-left) compared to the traditional Cox model without weights (bottom-right): estimates with respect to reference level improved even if statistical significance did not change, showing the bias due to *toxicity-treatment-adjustment*. Estimates for Cox MSM 2 (see Table 3) showed, for the same RDI level, that a *good* response caused an 83.8% decrease in the risk of an event ( $\exp(\hat{\beta}_3) = 0.162$ ) with respect to a *poor* one. Moreover, 1-unit increase in the number of reductions of 15-30% (i.e., 1-unit increase in cum( $\bar{a}_1$ )) caused a decrease of 16.5% in the risk of an event for PRs ( $\exp(\hat{\beta}_1) = 0.835$ ) and an increase of 24.1% for GRs ( $\exp(\hat{\beta}_1 + \hat{\beta}_3) = 1.241$ ).

A possible clinical explanation for these results might be due to the effect of chemotherapy on non-cancerous cells. By targeting a broad spectrum of cells, chemotherapy also damages the processes and mechanisms of the immune system that can detect and kill cancer cells. While in GRs this negative effect may be largely offset by the efficacy of the tumour therapy, in PRs – for whom chemotherapy is less effective – an increased RDI may be detrimental to survival due to the impact on the immune system.

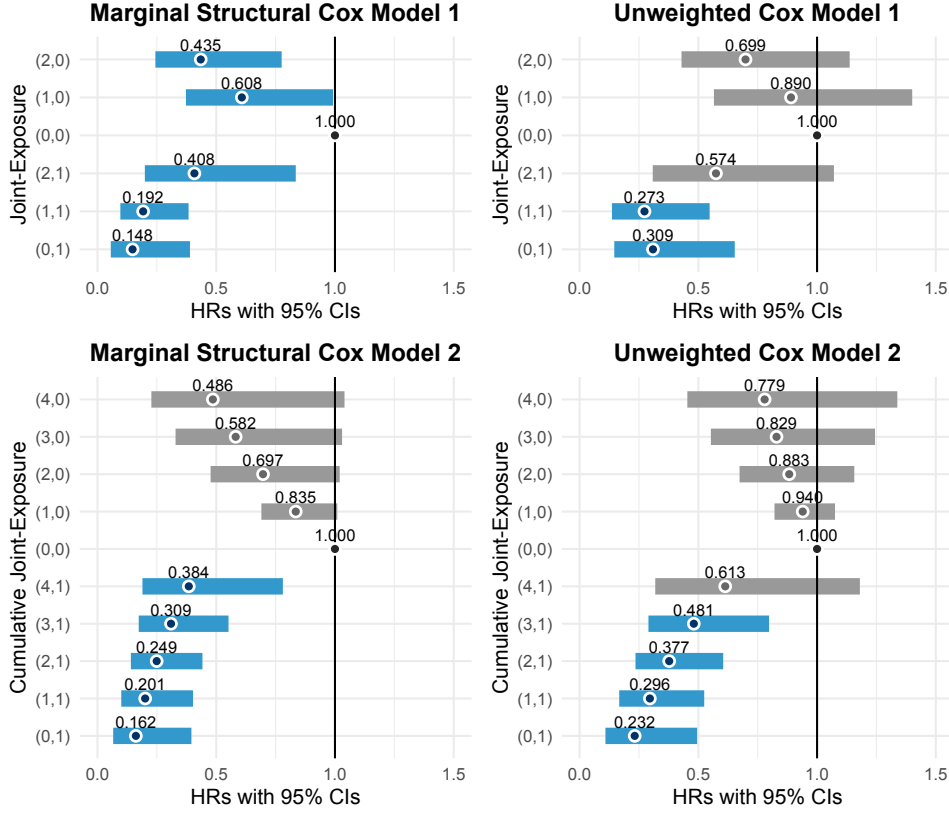


**Figure 10:** Graphical displays of Hazard Ratios (HRs) for different joint-exposures along with their 95% Confidence Intervals (CIs) for Marginal Structural Cox Models (left panels) and corresponding unweighted Cox models (right panels).

Top panels: Cox MSM 1 defined in Equation (6). Reference level is *poor* responder with *normal* RDI level at the end of treatment, i.e.,  $(a_1, a_2) = (0, 0)$ . The y-axis refers to *time-fixed joint-exposures*  $\mathbf{a} = (a_1, a_2)$ . Final RDI level  $a_1 \in \{0: \text{normal } RDI_i \geq 0.85; 1: \text{low-reduction } 0.70 \leq RDI_i < 0.85; 2: \text{high-reduction } RDI_i < 0.70\}$ ; HRe category  $a_2 \in \{0: \text{poor}; 1: \text{good}\}$ .

Bottom panels: Cox MSM 2 defined in Equation (10). Reference level is *poor* responder without reduction, i.e.,  $(\text{cum}(\bar{\mathbf{a}}_1), a_2) = (0, 0)$ . The y-axis refers to *cumulative joint-exposures*  $\bar{\mathbf{a}} = (\text{cum}(\bar{\mathbf{a}}_1), a_2)$ . Cumulative RDI level  $\text{cum}(\bar{\mathbf{a}}_1) \in \{0: \text{no reduction}; 1: \text{only one low reduction pre or post surgery}; 2: \text{low reductions both pre and post surgery or high reduction pre or post surgery}; 3: \text{one low reduction and one high reduction}; 4: \text{high reductions pre and post surgery}\}$ ; HRe category  $a_2 \in \{0: \text{poor}; 1: \text{good}\}$ .

## 5 Discussions

In cancer trials, longitudinal chemotherapy data are problematic to analyse due to the presence of negative feedback between exposure to cytotoxic drugs and consequent toxic side effects. Therapy administration is usually complicated by the dynamical adjustment of the treatment based on patients' clinical characteristics, in particular on chemotherapy-induced multi-systemic toxicities. For this reason, chemotherapy is usually modelled by Intention-To-Treat (ITT) analysis,<sup>6</sup> although the introduction of Received Dose Intensity (RDI)<sup>8</sup> marked a significant departure from ITT in the direction of a closer description of the actual clinical practice. The main issue in analysing actual treatment lies in the fact that toxicities act as time-dependent confounders for the effect

of chemotherapy intensity exposure on survival, determining the *toxicity-treatment-adjustment* bias if not properly considered. Novel methodologies are hence needed to control for exposure-affected (time-varying) toxicity confounding in longitudinal chemotherapy data. In addition, since the assignment of dose reductions/interruptions or delays in administration during treatment is determined not by individual toxicities but by the overall toxic burden for each patient, different types and number of side effects must be adequately summarized to be included in the analysis.

Motivated by a sharp yet delicate clinical question on the effect of treatment modifications on EFS in osteosarcoma patients, this paper proposed a novel approach to use Marginal Structural Models (MSMs) in combination with Inverse-Probability-of-Treatment Weighted (IPTW) estimators to assess the causal effects of chemotherapy intensity exposure seen in terms of both Histological Response (HRe) and RDI reductions compared to protocol. Unbiased estimates from MSMs relied on the four main assumptions presented in Section 3.2. Control arms data from BO03 and BO06 trials for osteosarcoma were analyzed. Since only the most severe side-effects were recorded in BO03, the analysis of such mixed longitudinal/non-longitudinal data required a careful combination of several methodologies to develop a new analytical strategy for the research question under study. Data complexity and causal assumptions call for a note of caution in proposing an innovative methodology that would take into account all aspects of chemotherapy process. First, pre and post-operative toxicity data were summarized using the new Multiple Overall Toxicity (MOTox) approach<sup>28</sup> based on most severe CTACE grades for *rule-specific* and *generic* side effects. This new approach allowed (i) to reduce the number of possible confounders combinations dealing with non-positivity and highly-correlated data, and (ii) to meet the clinical rationale of tailoring treatment according to the patient’s overall toxic burden in the presence of multiple toxic side effects. Then, two novel joint-exposure characterizations – which met *consistency* according to experts – were properly defined based on *time-fixed final RDI* or *time-dependent pre/post-operative RDI* combined with HRe. To identify all possible (time-dependent) confounders and their relationships with both joint-exposure and EFS outcome, two Direct Acyclic Graphs (DAGs) were defined, validating the assumption of *no unmeasured confounding*. Appropriate IPTW-based techniques and Cox MSMs, representing the causal RDI analogues of the ITT Cox model presented by Lewis *et al.* (2007),<sup>26</sup> were finally designed to mimic a randomized trial where the joint-exposure intensity was no longer confounded by toxicities. In the pseudo-population thus created, a crude analysis sufficed to estimate the causal effect of joint-exposure modifications on EFS.

Regardless of RDI-level, in both Cox MSMs *Good* Responders (GRs) showed a better EFS than *Poor* ones (PRs). This was not surprising because HRe is the strongest prognostic survival factor known to date in osteosarcoma.<sup>4</sup> Increasing RDI-reductions caused two opposite trends for PRs and GRs: the higher the reduction in final or pre/post-operative RDI, the better (worsen) was the EFS in PRs (GRs). Future studies should investigate this phenomenon.

This is the first study where a DAG was developed to analyse chemotherapy data by using mixed longitudinal/non-longitudinal information. The lack of longitudinal confounders in BO03 imposed the causal structures represented in Figure 6. The two DAGs relied on the assumption that the most severe CTCAE grades of each toxicity in pre and post-operative treatment predicted well the final and pre/post-operative RDI values, thus flattening the toxicity history. The use of the new MOTox approach allowed to show the potential pitfalls of a naive RDI-based analysis of chemotherapy data. When ITT models were translated into RDI-based ones by simply neglecting the role of toxicities, results were clearly affected by the *toxicity-treatment-adjustment* bias. The use of Cox MSMs allowed to model the contribution of patient’s toxicity history to EFS through the realisation of the (cumulative) joint-exposures. In other words, the use of IPTW-based Cox MSMs broke the feedback between side effects and therapy adjustments, yielding to unbiased estimates of the effect of treatment modifications on EFS and describing better the effect of low-intensity regimens.

To the best of our knowledge, this is the first study on IPTW-based techniques for osteosarcoma trial data which developed a novel approach to (i) take into account all the peculiar aspects of chemotherapy, and (ii) eliminate the *toxicity-treatment-adjustment* bias. This study showed the difficulty of analysing chemotherapy data on a RDI-based approach. The main contribution of this paper is the presentation of innovative analytical strategies for complex chemotherapy data. Tutorial-like explanations of the difficulties present in this context and detailed descriptions of the novel problem-solving strategies were provided. Focusing on unconventional RDI-based models rather than ITT approach, this study illustrated the key role played by toxicities in this transition and showed the detrimental effect of neglecting them in the analyses.

## Acknowledgments

The authors thank Medical Research Council in London for sharing the dataset used in this work and Dr. Jakob Anninga, MD, for the clinical suggestions.

## References

- <sup>1</sup> S. Smeland, S. S. Bielack, J. Whelan, M. Bernstein, P. Hogendoorn, M. D. Krailo, R. Gorlick, K. A. Janeway, F. C. Ingleby, J. Anninga, I. Antal, C. Arndt, K. Brown, T. Butterfass-Bahloul, G. Calaminus, M. Capra, C. Dhooge, M. Eriksson, A. M. Flanagan, G. Friedel, ..., and N. Marina. Survival and prognosis with osteosarcoma: outcomes in more than 2000 patients in the EURAMOS-1 (European and American Osteosarcoma Study) cohort. *European Journal of Cancer*, 109:36–50, 2019.
- <sup>2</sup> J. Ritter and S.S. Bielack. Osteosarcoma. *Annals of Oncology*, 21(suppl 7):vii320–vii325, 10 2010.
- <sup>3</sup> Jakob K. Anninga, Hans Gelderblom, Marta Fiocco, Judith R. Kroep, Antoni H.M. Taminiu, Pan-cras C.W. Hogendoorn, and R. Maarten Egeler. Chemotherapeutic adjuvant treatment for osteosarcoma: Where do we stand? *European Journal of Cancer*, 47(16):2431–2445, 2011.
- <sup>4</sup> M. W. Bishop, Y. C. Chang, M. D. Krailo, P. A. Meyers, A. J. Provisor, C. L. Schwartz, N. M. Marina, L. A. Teot, M. C. Gebhardt, R. Gorlick, K. A. Janeway, and A. J. Chou. Assessing the Prognostic Significance of Histologic Response in Osteosarcoma: A Comparison of Outcomes on CCG-782 and INT0133-A Report From the Children’s Oncology Group Bone Tumor Committee. *Pediatric blood & cancer*, 63(10):1737–1743, 2016.
- <sup>5</sup> C. Lancia, J. Anninga, M. R. Sydes, C. Spitoni, J. Whelan, P. C. W. Hogendoorn, H. Gelderblom, and M. Fiocco. Method to measure the mismatch between target and achieved received dose intensity of chemotherapy in cancer trials: a retrospective analysis of the MRC BO06 trial in osteosarcoma. *BMJ open*, 9(5), 2019.
- <sup>6</sup> S. K. Gupta. Intention-to-treat concept: A review. *Perspectives in clinical research*, 2(3):109–112, 2011.
- <sup>7</sup> C. Lancia, J. Anninga, M. R. Sydes, C. Spitoni, J. Whelan, P. C. W. Hogendoorn, H. Gelderblom, and M. Fiocco. A novel method to address the association between received dose intensity and survival outcome: benefits of approaching treatment intensification at a more individualised level in a trial of the European Osteosarcoma Intergroup. *Cancer chemotherapy and pharmacology*, 83(5):951–962, 2019.
- <sup>8</sup> W M Hryniuk and M Goodyear. The calculation of received dose intensity. *Journal of Clinical Oncology*, 8(12):1935–1937, 1990.
- <sup>9</sup> Carlo Lancia, Cristian Spitoni, Jakob Anninga, Jeremy Whelan, Matthew R Sydes, Gordana Jovic, and Marta Fiocco. Marginal structural models with dose-delay joint-exposure for assessing variations to chemotherapy intensity. *Statistical Methods in Medical Research*, 28(9):2787–2801, 2019. PMID: 29916309.
- <sup>10</sup> Robert L Souhami, Alan W Craft, Jan W Van der Eijken, Marianne Nooij, David Spooner, Vivien HC Bramwell, Rafal Wierzbicki, Archibald J Malcolm, Anne Kirkpatrick, Barbara M Uscinska, Martine Van Glabbeke, and David Machin. Randomised trial of two regimens of chemotherapy in operable osteosarcoma: a study of the European Osteosarcoma Intergroup. *The Lancet*, 350(9082):911–917, 1997.

- <sup>11</sup> D. R. Cox. Regression models and life-tables. *Journal of the Royal Statistical Society*, 34(2):187–220, 1972.
- <sup>12</sup> Terry Therneau and Patricia Grambsch. *Modeling survival data: Extending the Cox model*. Statistics for Biology and Health. Springer, New York, NY, 1 edition, 2010.
- <sup>13</sup> David G Kleinbaum and Mitchel Klein. *Survival Analysis*. Statistics for Biology and Health. Springer, New York, NY, 2016.
- <sup>14</sup> O. O. Aalen, R. J. Cook, and K. Røysland. Does Cox analysis of a randomized survival study yield a causal treatment effect? *Lifetime data analysis*, 21(4):579–593, 2015.
- <sup>15</sup> R. M. Daniel, S. N. Cousens, B. L. De Stavola, M. G. Kenward, and J. A. Sterne. Methods for dealing with time-dependent confounding. *Statistics in medicine*, 32(9):1584–1618, 2013.
- <sup>16</sup> James Robins. A new approach to causal inference in mortality studies with a sustained exposure period—application to control of the healthy worker survivor effect. *Mathematical Modelling*, 7(9):1393–1512, 1986.
- <sup>17</sup> J. M. Robins, D. Blevins, G. Ritter, and M. Wulfsohn. G-estimation of the effect of prophylaxis therapy for *Pneumocystis carinii* pneumonia on the survival of AIDS patients. *Epidemiology*, 3(4):319–336, 1992.
- <sup>18</sup> J. M. Robins, M. A. Hernán, and B. Brumback. Marginal structural models and causal inference in epidemiology. *Epidemiology*, 11(5):550–560, 2000.
- <sup>19</sup> P. J. Clare, T. A. Dobbins, and R. P. Mattick. Causal models adjusting for time-varying confounding—a systematic review of the literature. *International journal of epidemiology*, 48(1):254–265, 2019.
- <sup>20</sup> Miguel A Hernán, Babette Brumback, and James M Robins. Marginal Structural Models to Estimate the Causal Effect of Zidovudine on the Survival of HIV-Positive Men. *Epidemiology*, 11(5):561–570, 2000.
- <sup>21</sup> R. H. Keogh, S. R. Seaman, J. M. Gran, and S. Vansteelandt. Simulating longitudinal data from marginal structural models using the additive hazard model. *Biometrical Journal*, 63(7):1526–1541, 2021.
- <sup>22</sup> MA Hernán and JM Robins. *Causal Inference: What If*. 2020.
- <sup>23</sup> Stephen R. Cole and Miguel A. Hernán. Constructing Inverse Probability Weights for Marginal Structural Models. *American Journal of Epidemiology*, 168(6):656–664, 2008.
- <sup>24</sup> V. Allan, S. V. Ramagopalan, J. Mardekian, A. Jenkins, X. Li, X. Pan, and X. Luo. Propensity score matching and inverse probability of treatment weighting to address confounding by indication in comparative effectiveness research of oral anticoagulants. *Journal of comparative effectiveness research*, 9(9):603–614, 2020.
- <sup>25</sup> Ian J. Lewis, Simon Weeden, David Machin, Dan Stark, and Alan W. and Craft. Received Dose and Dose-Intensity of Chemotherapy and Outcome in Nonmetastatic Extremity Osteosarcoma. *Journal of Clinical Oncology*, 18(24):4028–4037, 2000.
- <sup>26</sup> I.J. Lewis, Marianne A. Nooij, Jeremy Whelan, Matthew R. Sydes, Robert Grimer, Pancras C. W. Hogendoorn, Muhammad A. Memon, Simon Weeden, Barbara M. Uscinska, Martine van Glabbeke, Anne Kirkpatrick, Esther I. Hauben, Alan W. Craft, Antonie H. M. Taminiau, and On behalf of MRC BO06 and EORTC 80931 collaborators and European Osteosarcoma Intergroup. Improvement in Histologic Response But Not Survival in Osteosarcoma Patients Treated With Intensified Chemotherapy: A Randomized Phase III Trial of the European Osteosarcoma Intergroup. *JNCI: Journal of the National Cancer Institute*, 99(2):112–128, 2007.
- <sup>27</sup> S. Greenland, J. Pearl, and J. M. Robins. Causal diagrams for epidemiologic research. *Epidemiology*, 10(1):37–48, 1999.
- <sup>28</sup> Marta Spreafico, Francesca Ieva, Francesca Arlati, Federico Capello, Federico Fatone, Filippo Fedeli, Gianmarco Genalti, Jakob Anninga, Hans Gelderblom, and Marta Fiocco. Novel longitudinal Multiple Overall Toxicity (MOTox) score to quantify adverse events experienced by patients during chemotherapy treatment: a retrospective analysis of the MRC BO06 trial in osteosarcoma. *BMJ Open*, 11(12):e053456, 2021.

- <sup>29</sup> G. Rosen and A. Nirenberg. Neoadjuvant chemotherapy for osteogenic sarcoma: a five year follow-up (T-10) and preliminary report of new studies (T-12). *Progress in clinical and biological research*, 201:39–51, 1985.
- <sup>30</sup> U.S. Department of Health and Human Services. *Common Terminology Criteria for Adverse Events v3.0 (CTCAE)*, 2006. <https://www.eortc.be/services/doc/ctc/ctcae3.pdf>.
- <sup>31</sup> M. Collins, M. Wilhelm, R. Conyers, A. Herschtal, J. Whelan, S. Bielack, L. Kager, T. Kühne, M. Sydes, H. Gelderblom, and Ferrari, S. and Picci, P. and Smeland, S. and Eriksson, M. and Petrilli, A. S. and Bleyer, A. and Thomas, D. M. Benefits and Adverse Events in Younger Versus Older Patients Receiving Neoadjuvant Chemotherapy for Osteosarcoma: Findings From a Meta-Analysis. *Journal of Clinical Oncology*, 31(18):2303–2312, 2013.
- <sup>32</sup> Miguel A Hernán, Babette Brumback, and James M Robins. Marginal Structural Models to Estimate the Joint Causal Effect of Nonrandomized Treatments. *Journal of the American Statistical Association*, 96(454):440–448, 2001.
- <sup>33</sup> Mohammad Ehsanul Karim, Paul Gustafson, John Petkau, Afsaneh Shirani Yinshan Zhao, Elaine Kingwell, Charity Evans, Mia van der Kop, Joel Oger, and Helen Tremlett. Marginal Structural Cox Models for Estimating the Association Between  $\beta$ -Interferon Exposure and Disease Progression in a Multiple Sclerosis Cohort. *American Journal of Epidemiology*, 180(2):160–171, 2014.
- <sup>34</sup> Tyler Williamson and Pietro Ravani. Marginal structural models in clinical research: when and how to use them? *Nephrology Dialysis Transplantation*, 32(suppl 2):ii84–ii90, 2017.
- <sup>35</sup> Stephen R Cole and Constantine E Frangakis. The Consistency Statement in Causal Inference. *Epidemiology*, 20(3-5), 2009.
- <sup>36</sup> Mohammad Ehsanul Karim, John Petkau, Paul Gustafson, Helen Tremlett, and The Beams Study Group. On the application of statistical learning approaches to construct inverse probability weights in marginal structural Cox models: Hedging against weight-model misspecification. *Communications in Statistics - Simulation and Computation*, 46(10):7668–7697, 2017.
- <sup>37</sup> Peter C. Austin and Elizabeth A. Stuart. Moving towards best practice when using inverse probability of treatment weighting (IPTW) using the propensity score to estimate causal treatment effects in observational studies. *Statistics in Medicine*, 34(28):3661–3679, 2015.
- <sup>38</sup> D. A. Binder. Fitting cox’s proportional hazards models to survey data. *Biometrika*, 79:139–147, 1992.
- <sup>39</sup> D. Y. Lin. On fitting Cox’s proportional hazards models to survey data. *Biometrika*, 87:37–47, 2000.
- <sup>40</sup> R Core Team. *R: A Language and Environment for Statistical Computing*. R Foundation for Statistical Computing, Vienna, Austria, 2021. <https://www.R-project.org/>.
- <sup>41</sup> Willem M. van der Wal and Ronald B. Geskus. ipw: An R package for inverse probability weighting. *Journal of Statistical Software*, 43(13):1–23, 2011.
- <sup>42</sup> T. Therneau. *A Package for Survival Analysis in R*. R package version 3.2-13, 2021. <https://www.R-project.org/package=survival>.
- <sup>43</sup> M. Schemper and T. L. Smith. A note on quantifying follow-up in studies of failure time. *Controlled Clinical Trials*, 17(4):343–346, 1996.

## Appendix

### A Flowchart BO03/BO06 cohort selection

Figure A.1 displays the consort diagram related to the final cohort of 276 patients (114 and 162 from BO03 and BO06, respectively) included in the analyses, as described in Section 2.1.

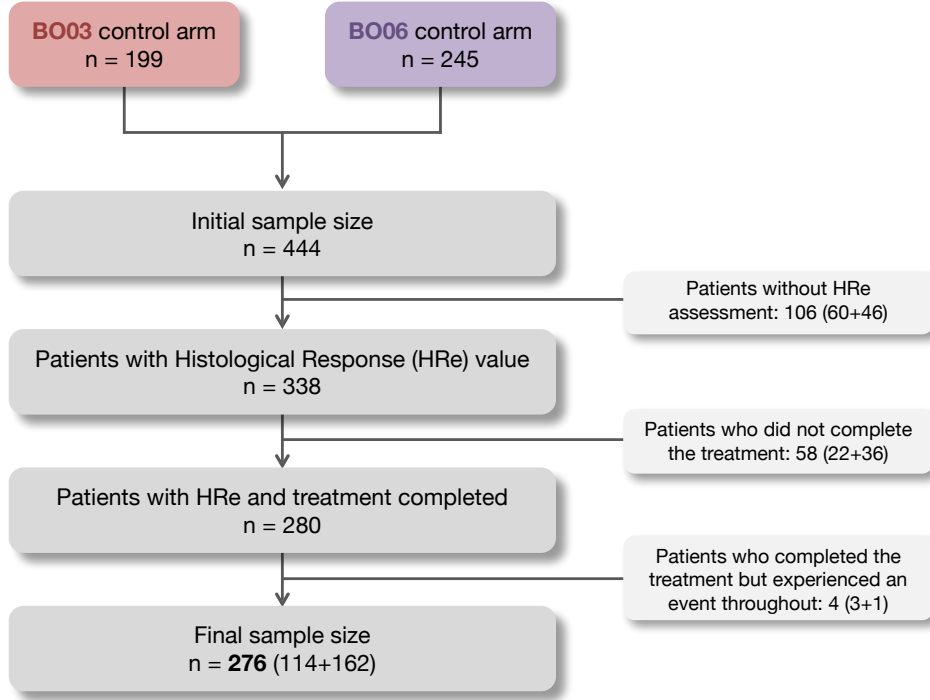


Figure A.1: Flowchart of cohort selection.

### B CTCAE grades specification for *rule-specific* and *generic* toxicities

In both BO03 and BO06 studies, toxic side effects were recorded using the Common Terminology Criteria for Adverse Events Version 3 (CTCAE v3.0),<sup>30</sup> with grades ranging from 0 (none) to 4 (life-threatening). In particular, Table B.1 reports the CTCAE-grades for *rule-specific* toxicities (i.e., *leucopenia*, *thrombocytopenia*, *oral mucositis*, *ototoxicity*, *cardiotoxicity* and *neurotoxicity*) and *generic* ones (i.e., *nausea/vomiting* and *infections*).

### C Pre/Post-operative Received Dose Intensity definitions

For each patient  $i$ , let  $np_i$  denote the number of cycles performed before the surgery. *Pre-operative* period is made up of cycles performed before surgery, i.e.,  $j \in \{1, \dots, np_i\}$ . *Post-operative* period is made up of cycles performed after surgery, i.e.,  $j \in \{np_i + 1, \dots, 6\}$ . To consider the two periods separately, definitions in Equations ((2)), ((3)) and ((4)) in Section 2.2.1 can be adapted as follows.

**Table B.1:** Toxicity coding based on Common Terminology Criteria for Adverse Events (CTCAE) v3.0 by<sup>30</sup> for *rule-specific* (i.e., leucopenia, thrombocytopenia, oral mucositis, ototoxicity, ototoxicity and neurotoxicity) and *generic* (i.e., nausea/vomiting and infections) toxicities.

<b>Toxicity</b>	<b>Grade 0</b>	<b>Grade 1</b>	<b>Grade 2</b>	<b>Grade 3</b>	<b>Grade 4</b>
<b><i>Rule-specific</i></b>					
<i>Leucopenia</i>	$\geq 4.0 \times 10^9/L$	$[3.0 - 4.0) \times 10^9/L$	$[2.0 - 3.0) \times 10^9/L$	$[1.0 - 2.0) \times 10^9/L$	$< 1.0 \times 10^9/L$
<i>Thrombocytopenia</i>	$\geq 100 \times 10^9/L$	$[75 - 100) \times 10^9/L$	$[50 - 75) \times 10^9/L$	$[25 - 50) \times 10^9/L$	$< 25 \times 10^9/L$
<i>Oral Mucositis</i>	No change	Soreness or erythema	Ulcers: can eat solid	Ulcers: liquid diet only	Alimentation not possible
<i>Cardiac toxicity</i>	No change	Sinus tachycardia	Unifocal PVC arrhythmia	Multifocal PVC	Ventricular tachycardia
<i>Ototoxicity</i>	No change	Slight hearing loss	Moderate hearing loss	Major hearing loss	Complete hearing loss
<i>Neurological toxicity</i>	None	Paraesthesia	Severe paraesthesia	Intolerable paraesthesia	Paralysis
<b><i>Generic</i></b>					
<i>Nausea/Vomiting</i>	None	Nausea	Transient vomiting	Continuative vomiting	Intractable vomiting
<i>Infection</i>	None	Minor infection	Moderate infection	Major infection	Major infection with hypotension

PVC = Premature Ventricular Contraction

**Pre/Post-operative standardized dose.** The pre-operative and post-operative standardized doses  $\Delta_{i,pre}$  and  $\Delta_{i,post}$  for patient  $i$  are defined as

$$\Delta_{i,pre} = \frac{1}{2} (\Delta_{i,pre}^{CDDP} + \Delta_{i,pre}^{DOX}) = \frac{1}{2 \cdot np_i} \left( \sum_{j=1}^{np_i} \delta_{ij}^{CDDP} + \sum_{j=1}^{np_i} \delta_{ij}^{DOX} \right),$$

$$\Delta_{i,post} = \frac{1}{2} (\Delta_{i,post}^{CDDP} + \Delta_{i,post}^{DOX}) = \frac{1}{2 \cdot (6 - np_i)} \left( \sum_{j=np_i+1}^6 \delta_{ij}^{CDDP} + \sum_{j=np_i+1}^6 \delta_{ij}^{DOX} \right).$$

**Pre/Post-operative standardized time.** The pre-operative standardized time for patient  $i$  is

$$\Gamma_{i,pre} = \frac{\text{actual pre-operative time}}{\text{anticipated pre-operative time}}$$

where

- *actual pre-operative time* is the difference in days between the starting date of cycle 1 and the date of the surgery,
- *anticipated pre-operative time* is  $21 \times np_i$  days, i.e.,  $np_i$  cycles lasting 21 days each.

Similarly, the post-operative standardized time for patient  $i$  is

$$\Gamma_{i,post} = \frac{\text{actual post-operative time}}{\text{anticipated post-operative time}}$$

where

- *actual post-operative time* is the difference in days between the surgery date and the 3rd day after the start of cycle 6,
- *anticipated post-operative time* is  $14 + (5 - np_i) \times 21 + 3$  days, i.e., 14 days of surgery,  $5 - np_i$  cycles lasting 21 days each and 3 days after the start of cycle 6.

**Pre/Post-operative Received Dose Intensity.** The pre-operative and post-operative Received Dose Intensities (RDIs) for patient  $i$  are defined as

$$RDI_{i,pre} = \frac{\Delta_{i,pre}}{\Gamma_{i,pre}}, \quad (13)$$

$$RDI_{i,post} = \frac{\Delta_{i,post}}{\Gamma_{i,post}}. \quad (14)$$

The RDI computed on the whole treatment as in Equation (3) is not the sum of pre-operative and post-operative RDIs, i.e.,  $RDI_i \neq RDI_{i,pre} + RDI_{i,post}$ .

A summary of  $RDI_{i,pre}$  and  $RDI_{i,post}$  exposure characteristics for the whole cohort and conditional on trials is reported in Figure 4. Figure C.1 shows the scatter plots of pre- (top panels) and post- (bottom panels) operative RDI ( $RDI_{i,k}$ ) against their relative standardized doses of CDDP+DOX ( $\Delta_{i,k}$ ) conditional on trial (left panel: *BO03*; right panel: *BO06*) and HRe (blue: *poor*; green: *good*). The solid horizontal lines in pink vertically divide patients with *normal* RDI levels ( $RDI_{i,k} \geq 0.85$ ) from *low* reduction ( $0.70 \leq RDI_{i,k} < 0.85$ ) and *high* reduction ( $RDI_{i,k} < 0.70$ ) patients. The solid diagonal line in black satisfies equation  $RDI_{i,k} = \Delta_{i,k}$ , dividing the group of patients with standardized time  $\Gamma_{i,k} > 1$  (delayed therapy, below the line)

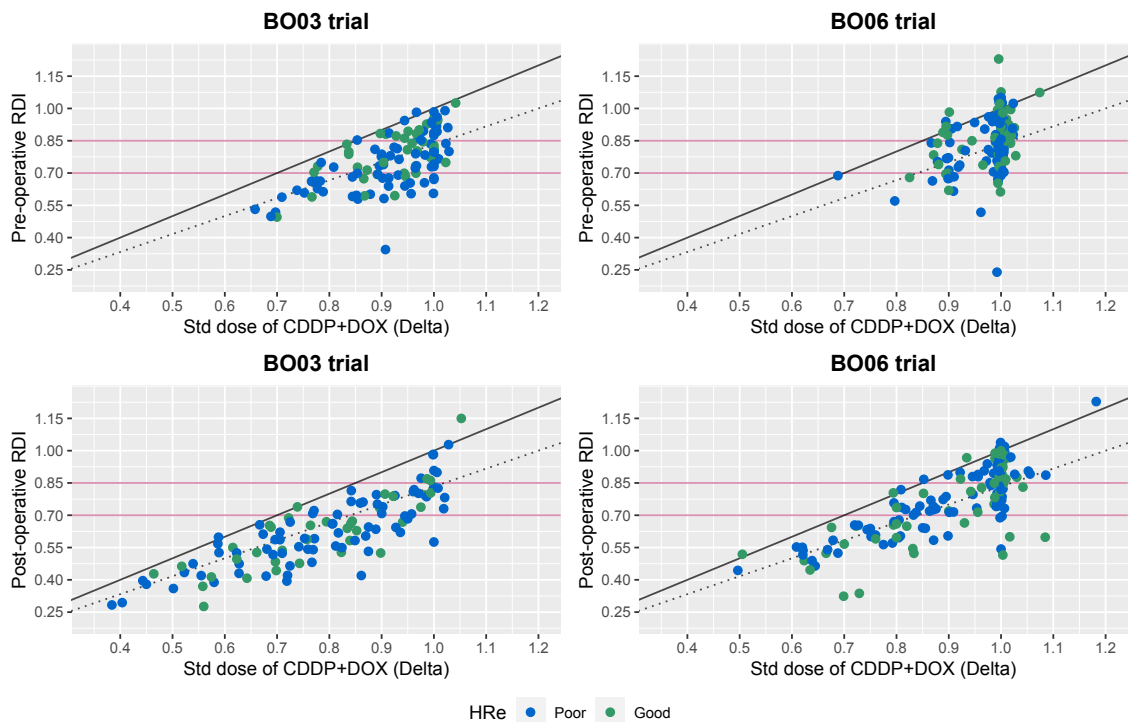


**Figure C.1:** Top panels: Scatter plots of pre-operative RDI (i.e.,  $RDI_{i,pre}$  in Equation (??)) against pre-operative standardized dose of CDDP+DOX ( $\Delta_{i,pre}$ ) conditional on trial (*BO03*: left panel; *BO06*: right panel) and HRe (*poor*: blue; *good*: green). Bottom panels: Scatter plots of post-operative RDI (i.e.,  $RDI_{i,post}$  in Equation (??)) against post-operative standardized dose of CDDP+DOX ( $\Delta_{i,post}$ ) conditional on trial (*BO03*: left panel; *BO06*: right panel) and HRe (*poor*: blue; *good*: green).

from the group, almost void, of patients with  $\Gamma_{i,k} < 1$  (anticipated therapy, above the line). The dotted diagonal line in black satisfies equation  $RDI_{i,k} = \Delta_{i,k}/1.2$ , dividing the group of patients with therapy delayed by more than 20% of anticipated time (below the dotted line) from the group of patients with therapy delayed by less than 20% of anticipated time (between solid and dotted black lines). This figure clearly shows the difference of treatment delivery in *BO03* vs. *BO06*, also considering pre/post-operative periods separately. It also shows the lack of a clear association between HRe and pre/post-operative RDI.

## D Denominator specifications for selected IPTW models

In Section 4.2, different model specifications (in terms of confounding covariates  $L$  for the denominators) to determine the subject-specific standardized weights for

- final RDI level  $SW_i^{A^1}$ ,
- HRe category  $SW_i^{A^2}$ ,
- pre/post-operative RDI levels  $SW_i^{\bar{A}^1} = SW_i^{A^1_{pre}} \cdot SW_i^{A^1_{post}}$

were investigated.

The following denominator formulas were selected:

- multinomial logistic regression model for denominator of final RDI level  $SW_i^{A^1}$ :

$$\log \frac{\Pr(A_i^1 = a | \mathbf{L}_i^1)}{\Pr(A_i^1 = 0 | \mathbf{L}_i^1)} = \gamma_{a0} + \gamma_{a1} \cdot \mathbb{1}_{(\text{trial}_i = BO06)} + \gamma_{a2} \cdot \mathbb{1}_{(\text{age}_i = \text{adolescent})} + \gamma_{a3} \cdot \mathbb{1}_{(\text{age}_i = \text{adult})} + \\ \gamma_{a4} \cdot \mathbb{1}_{(\text{gender}_i = \text{male})} + \gamma_{a5} \cdot \text{MOTox}_{i,\text{pre}}^{(\text{gen})} + \gamma_{a6} \cdot \text{MOTox}_{i,\text{pre}}^{(\text{rule})} + \\ \gamma_{a7} \cdot \text{MOTox}_{i,\text{post}}^{(\text{gen})} + \gamma_{a8} \cdot \text{MOTox}_{i,\text{post}}^{(\text{rule})}$$

where confounding covariates are

$$\mathbf{L}_i^1 = \left( \mathbf{L}_i^{\text{base}}, \mathbf{L}_{i,\text{pre}}^{\text{tox}}, \mathbf{L}_{i,\text{post}}^{\text{tox}} \right) \\ = \left( \text{trial}_i, \text{age}_i, \text{gender}_i, \text{MOTox}_{i,\text{pre}}^{(\text{gen})}, \text{MOTox}_{i,\text{pre}}^{(\text{rule})}, \text{MOTox}_{i,\text{post}}^{(\text{gen})}, \text{MOTox}_{i,\text{post}}^{(\text{rule})} \right);$$

- binary logistic regression model for denominator of HRe category  $SW_i^{A^2}$

$$\log \frac{\Pr(A_i^2 = 1 | \mathbf{L}_i^2)}{1 - \Pr(A_i^2 = 1 | \mathbf{L}_i^2)} = \alpha_0 + \alpha_1 \cdot \mathbb{1}_{(\text{trial}_i = BO06)} + \alpha_2 \cdot \mathbb{1}_{(\text{age}_i = \text{adolescent})} + \alpha_3 \cdot \mathbb{1}_{(\text{age}_i = \text{adult})} + \\ \alpha_4 \cdot \mathbb{1}_{(\text{gender}_i = \text{male})} + \alpha_5 \cdot \text{MOTox}_{i,\text{pre}}^{(\text{gen})} + \alpha_6 \cdot \text{MOTox}_{i,\text{pre}}^{(\text{rule})} + \\ \alpha_7 \cdot \mathbb{1}_{(\text{surgery}_i = \text{on time})}$$

where confounding covariates are

$$\mathbf{L}_i^2 = \left( \mathbf{L}_i^{\text{base}}, \mathbf{L}_{i,\text{pre}}^{\text{tox}}, \mathbf{L}_i^{\text{surrg}} \right) = \left( \text{trial}_i, \text{age}_i, \text{gender}_i, \text{MOTox}_{i,\text{pre}}^{(\text{gen})}, \text{MOTox}_{i,\text{pre}}^{(\text{rule})}, \text{surgery}_i \right);$$

- multinomial logistic regression model for denominator of pre-operative RDI level  $SW_i^{A^1_{\text{pre}}}$ :

$$\log \frac{\Pr(A_{i,\text{pre}}^1 = a | \mathbf{L}_{i,\text{pre}}^1)}{\Pr(A_{i,\text{pre}}^1 = 0 | \mathbf{L}_{i,\text{pre}}^1)} = \gamma_{a0} + \gamma_{a1} \cdot \mathbb{1}_{(\text{trial}_i = BO06)} + \gamma_{a2} \cdot \mathbb{1}_{(\text{age}_i = \text{adolescent})} + \\ \gamma_{a3} \cdot \mathbb{1}_{(\text{age}_i = \text{adult})} + \gamma_{a4} \cdot \mathbb{1}_{(\text{gender}_i = \text{male})} + \gamma_{a5} \cdot \text{MOTox}_{i,\text{pre}}^{(\text{gen})} + \\ \gamma_{a6} \cdot \text{MOTox}_{i,\text{pre}}^{(\text{rule})}$$

where confounding covariates are

$$\mathbf{L}_{i,\text{pre}}^1 = \left( \mathbf{L}_i^{\text{base}}, \mathbf{L}_{i,\text{pre}}^{\text{tox}} \right) = \left( \text{trial}_i, \text{age}_i, \text{gender}_i, \text{MOTox}_{i,\text{pre}}^{(\text{gen})}, \text{MOTox}_{i,\text{pre}}^{(\text{rule})} \right);$$

- multinomial logistic regression model for denominator of post-operative RDI level  $SW_i^{A^1_{\text{post}}}$ :

$$\log \frac{\Pr(A_{i,\text{post}}^1 = a | \bar{\mathbf{L}}_{i,\text{post}}^1, A_{i,\text{pre}}^1)}{\Pr(A_{i,\text{post}}^1 = 0 | \bar{\mathbf{L}}_{i,\text{post}}^1, A_{i,\text{pre}}^1)} = \gamma_{a0} + \gamma_{a1} \cdot \mathbb{1}_{(\text{trial}_i = BO06)} + \gamma_{a2} \cdot \mathbb{1}_{(\text{age}_i = \text{adolescent})} + \\ \gamma_{a3} \cdot \mathbb{1}_{(\text{age}_i = \text{adult})} + \gamma_{a4} \cdot \mathbb{1}_{(\text{gender}_i = \text{male})} + \gamma_{a5} \cdot \text{MOTox}_{i,\text{pre}}^{(\text{gen})} + \\ \gamma_{a6} \cdot \text{MOTox}_{i,\text{pre}}^{(\text{rule})} + \gamma_{a7} \cdot \mathbb{1}_{(A_{i,\text{pre}}^1 = 1)} + \gamma_{a8} \cdot \mathbb{1}_{(A_{i,\text{pre}}^1 = 2)} + \\ \gamma_{a9} \cdot \text{MOTox}_{i,\text{post}}^{(\text{gen})} + \gamma_{a10} \cdot \text{MOTox}_{i,\text{post}}^{(\text{rule})}.$$

where  $A_{i,pre}^1$  is the pre-operative RDI level and confounding covariates are

$$\begin{aligned}\bar{\mathbf{L}}_{i,post}^1 &= (\mathbf{L}_i^{base}, \mathbf{L}_{i,pre}^{tox}, \mathbf{L}_{i,post}^{tox}) \\ &= (\text{trial}_i, \text{age}_i, \text{gender}_i, \text{MOTox}_{i,pre}^{(gen)}, \text{MOTox}_{i,pre}^{(rule)}, \text{MOTox}_{i,post}^{(gen)}, \text{MOTox}_{i,post}^{(rule)}).\end{aligned}$$